Response of Continuous CFRP Prestressed Concrete Bridges Under Static and Repeated Loadings

Nabil F. Grace, Ph.D, P.E.
Professor and Director of Structural Testing Center
Civil Engineering Department
Lawrence Technological University
Southfield, Michigan

A detailed experimental investigation of a developed continuous double-T (DT) bridge system, internally and externally prestressed with carbon fiber reinforced polymer (CFRP) tendons, was conducted under static, repeated, and ultimate loads. The bridge model was subjected to 15 million cycles of two repeated loads of constant amplitudes equivalent to the service load at Midspan 1 and twice the service load at Midspan 2. The effect of repeated loads on various parameters was examined before and after the post-tensioning adjustment (increase in the post-tensioning forces after 7.5 million cycles of repeated loads). It is observed that the effect of repeated loads on the forces in post-tensioned externally draped tendons is negligible. However, the effect of repeated loads on other parameters such as deflection and strain depends on the magnitude of repeated loads and becomes more significant under loads greater than the service load. Also, the presence of continuous externally draped CFRP tendons (in the positive and negative moment regions), along with CFRP grids, results in a ductile CFRP continuous bridge system.

Because of its high specific strength (strength-to-weight ratio) and non-corrosive characteristics, interest in using carbon fiber reinforced polymer (CFRP) prestressing tendons in place of steel strands in concrete bridges is increasing rapidly. Small sections of bridges, as well as full bridges, have been built in different parts of the world.[1-5]

It has also been found from early research investigations[6-8] that internally bonded tendons in combination with externally unbonded tendons in simply supported bridges lead to a reasonably ductile bridge system. However, after an extensive literature review, it was concluded that little work has been conducted on the use of CFRP tendons in continuous prestressed concrete bridges.

The experimental CFRP prestressed concrete bridges constructed in different parts of the world demonstrate the successful use of CFRP tendons in simply supported bridges[2] only.

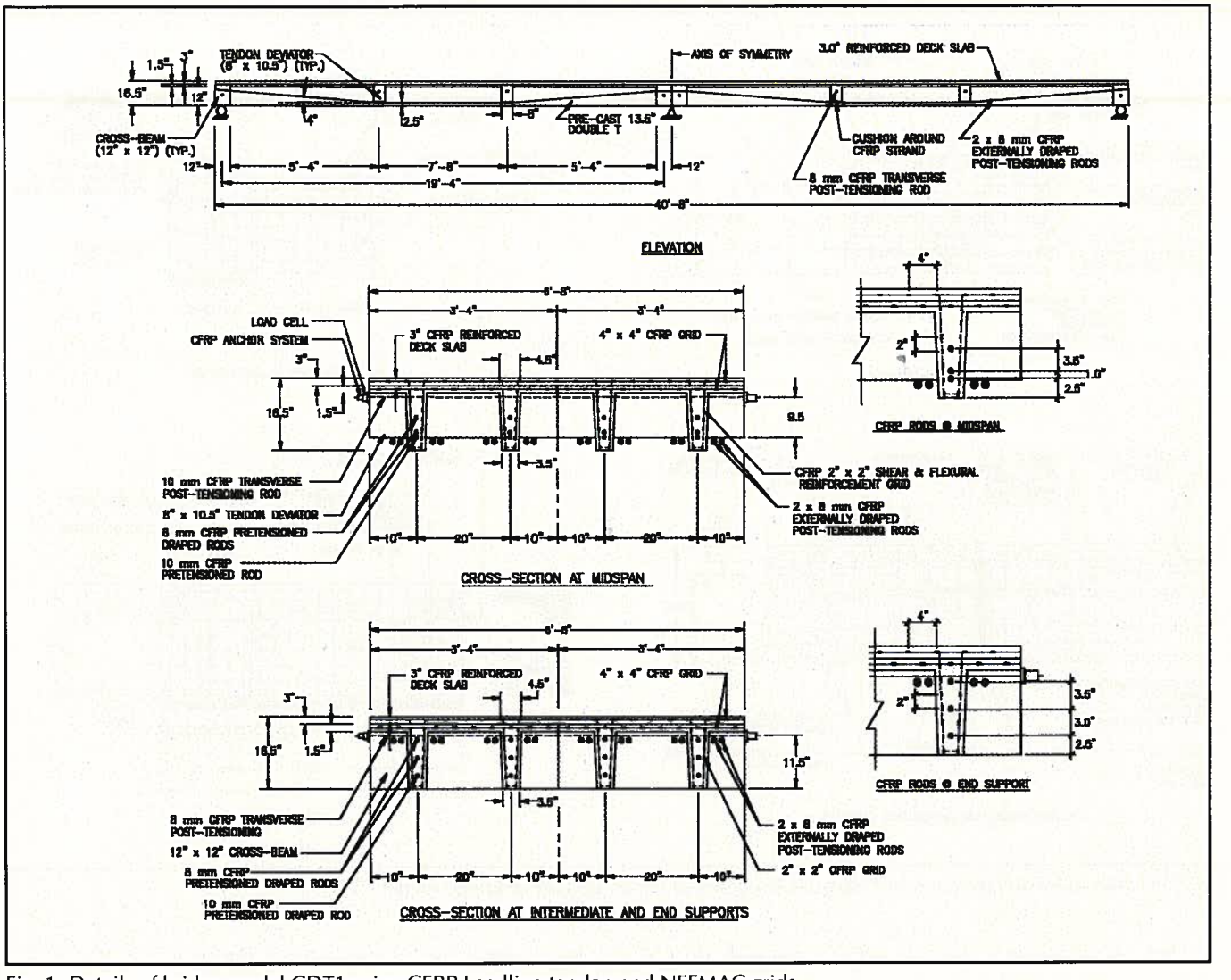

Fig. 1. Details of bridge model CDT1 using CFRP Leadline tendon and NEFMAC grids.

Therefore, it was logical to examine the applicability of continuous externally draped CFRP tendons in multispan continuous prestressed concrete bridges.

The basic question that the present investigation is trying to answer is: whether it is feasible to drape and post-tension CFRP tendons from the sagging moment region (midspan, i.e., positive moment) to the hogging moment zone (intermediate support, i.e., negative moment) and back to the sagging moment region in multispan continuous bridges?

To answer this question, a continuous (two-span) double-T bridge model CDT1 was developed and a thorough experimental investigation was conducted to determine the strain distribution at critical sections along the entire length of the bridge. Also, the effect of pretensioning of girders, placement of deck slab and post-tensioning of continuous externally draped tendons on the concrete strains and strain distribution throughout the depth of the bridge cross section were examined during these construction stages.

The deflection and strain responses of a simply supported bridge using the same construction components can be found in the work of Grace et al.,[9] wherein a mathematical solution is suggested for predicting the response of right and skew-angled CFRP prestressed concrete bridges. This mathematical solution is based on the assumption that the bridge behaves as an orthotropic plate and the effect of longitudinal and transverse prestressing forces can be implemented with the membrane theory concept.

Thus, the present study is an extension of previous work[6-8, 10-11] and aims at examining the response of a multispan continuous double-T CFRP prestressed bridge system under static, repeated (15 million cycles), and ultimate loads. The effect of repeated loading on various parameters such as post-tensioning forces in the continuous externally draped tendons, midspan deflections and concrete strains is examined before (0 to 7.5 million cycles) and after (7.5 to 15 million cycles) the post-tensioning adjustment (that is, the increase in post-tensioning forces).

BRIDGE SYSTEM DETAILS

Details of the bridge system and its construction are given elsewhere.[11] However, for the sake of completeness, they are also presented here. The two-span continuous CFRP prestressed concrete bridge primarily consists of the following:

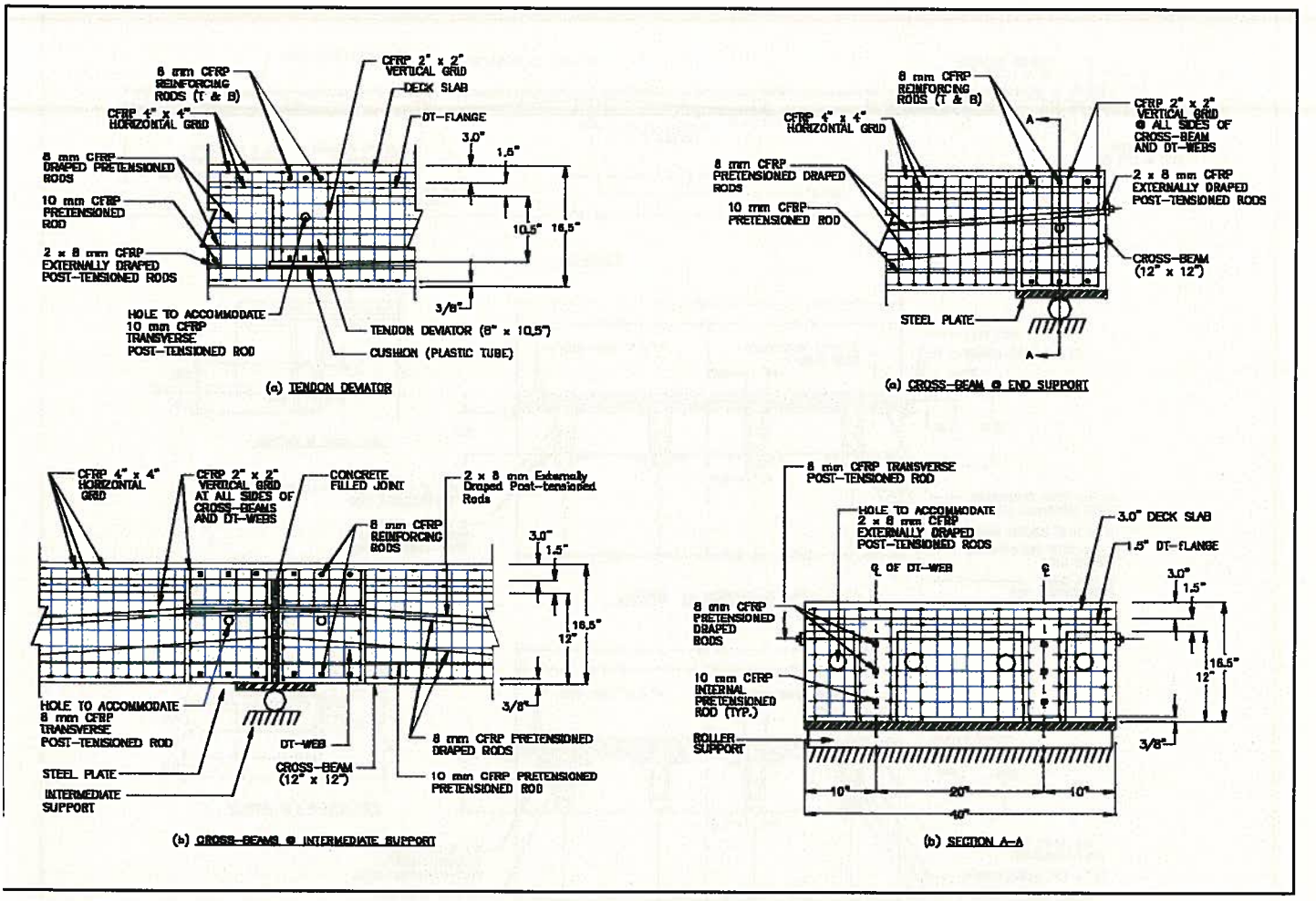

Fig. 2. Details of tendon deviator and cross-beams at intermediate support of bridge model CDT1.

1. Precast modified double-tee (DT) girders [to be used as simply supported girders] prestressed with straight and draped internally bonded Leadline™,* [12] tendons.

2. Transverse (unbonded) CFRP tendons post-tensioned through tendon deviators and cross-beams.

3. CFRP reinforced concrete deck slab.

4. CFRP three-dimensional grids[13] which project beyond the top flanges of the DT girders, cross-beams and tendon deviators.

5. Continuous externally draped CFRP Leadline tendons.

Details of bridge model CDT1, which uses CFRP Leadline tendons and three-dimensional CFRP-NEFMAC™,† grids, are shown in Fig. 1, while details of the tendon deviators and cross-beams at the intermediate support are shown in Fig. 2. Thus, in the developed bridge system, conventional steel flexural and shear reinforcements are replaced with NEFMAC grids.

The hold-up and hold-down devices used to develop the desired draped profile of CFRP Leadline tendons are made of stainless steel. Also, it should be noted that continuous externally draped tendons were used to provide continuous prestressing in the positive and negative moment regions.

Construction Details

Test Girders— Four double-T (DT) girders, designated as CDT1-1, CDT1-2, CDT1-3 and CDT1-4, were fabricated and prestressed with CFRP Leadline tendons. The material properties of the Leadline tendons are given in Table 1. In this notation, CDT stands for the Continuous Double-T bridge system; the first digit refers to the type of strand used (in this paper it is a Leadline tendon) and the last digit refers to the DT girder number. Tendon deviators (located approximately at the quarter points of each span) and cross-beams (located at each support) are integral parts of the DT girders.

The span of each girder is 19.33 ft (5.89 m). Each girder is 13.5 in. (345 mm) deep and its flange is 40 in. (1015 mm) wide. The center-to-center distance between the two webs of each DT girder is 20 in. (510 mm) and the thickness of the flange is 1.5 in. (38 mm). The widths of each web at the bottom and at the flange of a DT girder are 3.5 and 4.5 in. (90 and 115 mm), respectively.

Six tendons per DT girder were pretensioned prior to placing the concrete. In each web, each of the two top (draped) Leadline tendons is 0.3 in. (8 mm) in diameter while the bottom tendon (straight) is 0.4 in. (10 mm) in diameter. Details of prestressing, formwork, and other related construction procedures can be found elsewhere.[14]

"TM" refers to the trade mark name.
* Mitsubishi Chemical Corporation, Japan.
† Provided by Autocon Composites Incorporated, Canada.[13]

Reinforcement Details in the Girders— Four CFRP reinforcing cages were also fabricated using "NEFMAC" grids for flexural and shear reinforcement of the DT girder. Note that the size of each grid in the flange portion is 4 x 4 in. (100 x 100 mm) while in the web portion, each grid is 2 x 2 in. (50 x 50 mm) in size. Details of the layouts of the reinforcing cages and multi-use forms fabricated to produce DT girders are shown elsewhere.[11]

Pretensioning and Release of Prestressing Force— The desired draped[11] profile in the top two tendons was achieved by hold-up and hold-down devices. Each tendon was pretensioned by means of a hydraulic jack. The range of prestressing force varied from 60 to 70 percent of the guaranteed strength of the tendon. A saw cutting[14] approach was used to release the prestressing forces. First, the top pair of draped tendons (one in each web) was simultaneously released at both the live and dead ends. Next, a second pair of tendons was released. The bottom tendons were released last.

The average prestressing force in the draped tendons was approximately 17 kips (76 kN). For the straight tendons, it was approximately 19 kips (85 kN). This led to an average stress of 239 and 170 ksi (1650 and 1170 MPa) for the 0.3 and 0.4 in. (8 and 10 mm) diameter tendons, respectively.

Table 1. Characteristics of Leadline[12] tendons.

Characteristic	Specification
Matrix	Epoxy
Carbon fiber volume fraction	65
Tensile strength ksi (kN/mm^2)	328 (2.25)
Young's modulus ksi (GPa)	21320 (147)
Extension at break (percent)	1.5
Specific gravity	1.6
Relaxation ratio (percent)	2.3
Thermal expansion (1/°C)	0.68 x 10^{-6}
Effective cross-sectional area of 8 mm diameter tendon, sq in. (mm^2)	0.071 (46.1), [0.111 (71.8)]*
Guaranteed tensile strength for 8 mm diameter tendon, kips (kN)	23.4 (104), [36.4 (162)]*

* Refers to the tendon of 10 mm diameter.

Construction of Bridge Model CDT1

Each of the four DT girders fabricated earlier was transported to the testing area and positioned over the supports as a simply supported girder. An epoxy grout (Sikadur 30) was used to fill the gap at the joints between the DT girders. The total width of the bridge model was 6.66 ft (2.03 m) and each span was 19.33 ft (5.89 m).

Two continuous externally draped tendons [each 0.3 in. (8 mm) in diameter] within one anchor head assembly[8] were provided on both sides of each web for external post-tensioned prestressing of the bridge model. The 0.4 in. (10 mm) diameter tendons were used for transverse post-tensioned prestressing. Two stages of post-tensioning were applied for the external and transverse prestressing. In the first stage, 10 and 50 percent of the desired post-tensioning forces in the continuous externally draped tendons and in the tendons for transverse prestressing, respectively, were applied.

This partial prestressing in the longitudinal and transverse directions was intended to ensure that the four DT girders formed a tight platform for the deck slab. Cushioning materials between the tendons and the concrete at the tendon deviators and crossbeams were used to ensure successful performance[7] of the externally draped tendons.

The form of the deck slab was assembled and CFRP grids [4 x 4 in. (100 x 100 mm) spacing] for flexural reinforcements were used. The concrete mix [specified compressive strength of 7 ksi (48 MPa)] used in the deck slab was the same as utilized for the DT girders. After curing the concrete of the deck slab, the externally draped continuous tendons were retensioned to the desired prestressing force of 17.5 kips (78 kN) per prestressing tendon set. The post-tensioning in the transverse direction was then performed for a total force of 10 kips (45 kN) per tendon.

A typical arrangement of the continuous externally draped tendons after the post-tensioning (as seen from below) is shown in Fig. 3. Also, the initial post-tensioning forces were

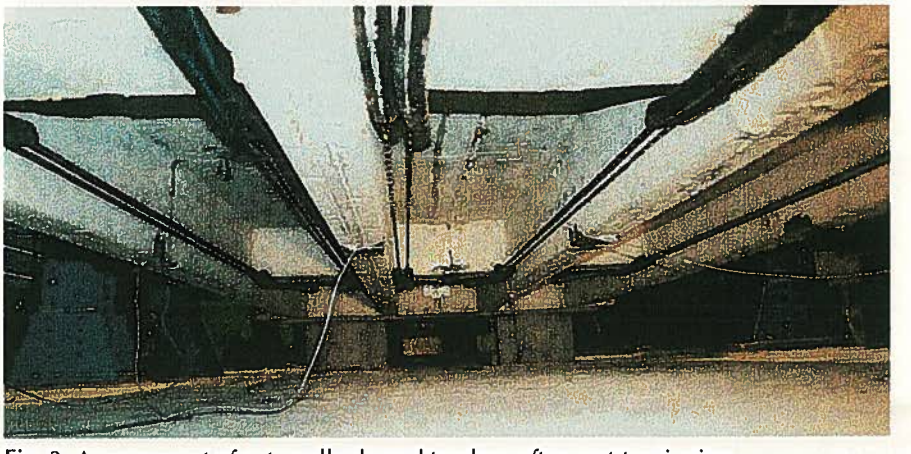

Fig. 3. Arrangement of externally draped tendons after post-tensioning.

Table 2. Average post-tensioning forces of externally draped CFRP tendons.

Initial post-tensioning at zero cycles			Adjusted (increased) post-tensioning force at 7.5 million cycles		
Post-tensioning force kips (kN)	Stress ksi (MPa)	Elongation in. (mm)	Post-tensioning force kips (kN)	Stress ksi (MPa)	Elongation in. (mm)
17.5	123 (845.0)	2.8 (72)	23.1 (102.7)	161 (1113)	3.9 (98)

readjusted (increased) during the testing stage of the bridge model, after the bridge is subjected to 7.5 million cycles of repeated loads. This will be discussed in the following section. The average values of the post-tensioning forces (initial and adjusted), stresses, and elongation in each pair of external prestressing tendons (placed on each side of each web) are presented in Table 2.

Instrumentation, Loading Setup and Data Acquisition

Load controlled MTS actuators were used to apply static and repeated loads to the bridge model (see Fig. 4) using a four-point loading system resembling the front and rear axles of a truck at each span. It was decided to simulate a lightweight truck of 19 kips (84.55 kN) in Span 1 and a heavy truck of 40 kips (178 kN) in Span 2. Repeated cyclic loads ranged from 2 to 21 kips (8.9 to 93.45 kN) on Span 1 and 5 to 45 kips (22.25 to 200.25 kN) on Span 2. Note that the 19 kip (84.55 kN) load simulates the service load while the 40 kip (178 kN) load simulates about twice the service load.

These two repeated loads were selected to evaluate the performance of the developed bridge in order to examine the effect of a service load and an overload of 15 million cycles. Also, suggested techniques were developed to regain the strength of an overloaded bridge if any adverse effect on the strength of the bridge system was observed. The frequency of the repeated loads was 2.5 Hz.

Note that in Span 1, a 200 kip (890 kN) static loading cylinder [24 in. (610 mm) off midspan] was used to apply the static load, ranging from 0 to 50 kips (222.5 kN). The actuator used for the repeated loading at Span 1 only had a capacity of 22 kips (97.90 kN).

A static load test was conducted after every one million cycles of repeated loading. Parameters such as deflections, strains and post-tensioning forces were recorded at each increment/decrement of 5 kips (22.25 kN) during loading/unloading of static loads. Post-tensioning forces in the continuous externally draped tendons and transverse prestressing tendons were monitored by load cells attached at their dead ends.

Note that the deflection measurements were taken using Linear Motion Transducers (LMT) located along the lengths of both spans and along their widths at midspan, while strain measurements were made by electrical resistance strain gauges.

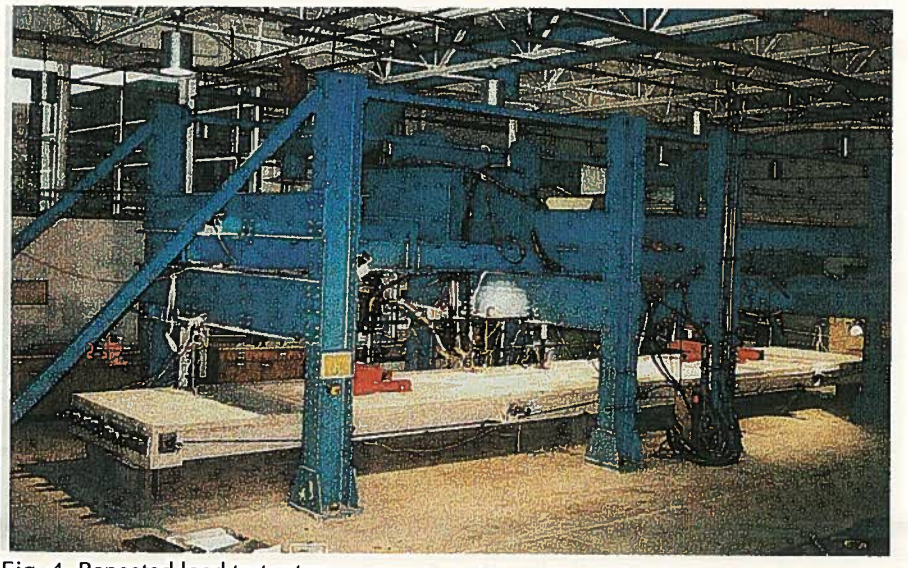

Fig. 4. Repeated load test setup.

DISCUSSION OF TEST RESULTS

Significant aspects of the test results are discussed below.

Strain Distributions

Fig. 5 shows the strain distributions at the top of the flanges and at the bottom of the webs for the intermediate support and Midspan 2 at three typical stages of construction, namely, pretensioning of internal CFRP tendons, placement of deck slab, and post-tensioning of external tendons. Note that the strains shown (after the addition of the deck slab) at the top of the deck slab refer to those strains at the top of the flanges of the girders.

The strains in the concrete at the top and bottom of the girders are compressive before and after placement of the deck slab. However, post-tensioning of the externally draped tendons causes a further increase in the compressive strain at the bottom of the girder but a small tensile strain at the top of the deck slab (at midspan). Note that the opposite is true at the intermediate support.

Thus, from these strain distributions, it is apparent that the strains developed at the top and bottom of the bridge after post-tensioning of the externally draped tendons are opposite in sign to those strains which will be caused by superposition of live loads. This is a desired result since the sections are maintained in pure compression even with the added tensile strains caused by live loads. Thus, no tensile cracks develop under service loads.

Post-Tensioning Forces Under Repeated Loading

In order to examine whether the lifespan of the developed bridge system can be increased with an increase in the post-tensioning forces at a particular age of the bridge, it was planned to apply repeated loads from 0 to 7.5 million cycles and increase (adjust) post-tensioning forces in the externally draped tendons by about 31.5 percent. This adjustment would restore any loss in parametric values such as deflection and strain. The bridge model was then tested again for an additional 7.5 million cycles, subjecting the structure to a total of 15 million cycles.

A typical variation in the post-tensioning forces (before and after the post-tensioning adjustment) in pairs X1-a, X1-b, X2-a, X2-b, X3-a, X3-b, X4-a and X4-b of post-tensioning CFRP tendons is shown in Fig. 6. Note that the post-tensioning forces are not influenced by the repeated load for 0 to 7.5 million cycles.

A similar observation is made after the post-tensioning adjustment, i.e., for 7.5 to 15 million cycles. Thus, post-tensioning forces remain stable over a large number (15 million) of cycles and, hence, there is no effect of fatigue on the post-tensioning forces in the continuous draped tendons.

STATIC RESPONSE I

In order to examine the effect of repeated loading before the post-tensioning adjustment on the response of the bridge under static loading conditions, the static load was applied from 0 to 50 kips (222.5 kN) in increments of 5 kips (22.25 kN). The bridge was then unloaded in decrements of 5 kips (22.25 kN) from 50 to 0 kips (222.5 to 0 kN) after the bridge was subjected to a number of cycles (varying from 0 to 7.5 million) of repeated loads.

At each increment/decrement of load, parameters such as deflections, strains, and post-tensioning forces were measured. Typical cases of variations in these parameters with static loads for different numbers of cycles are shown in Figs. 7 and 8.

Load versus Deflection

The load versus deflection relationship after the bridge model had been

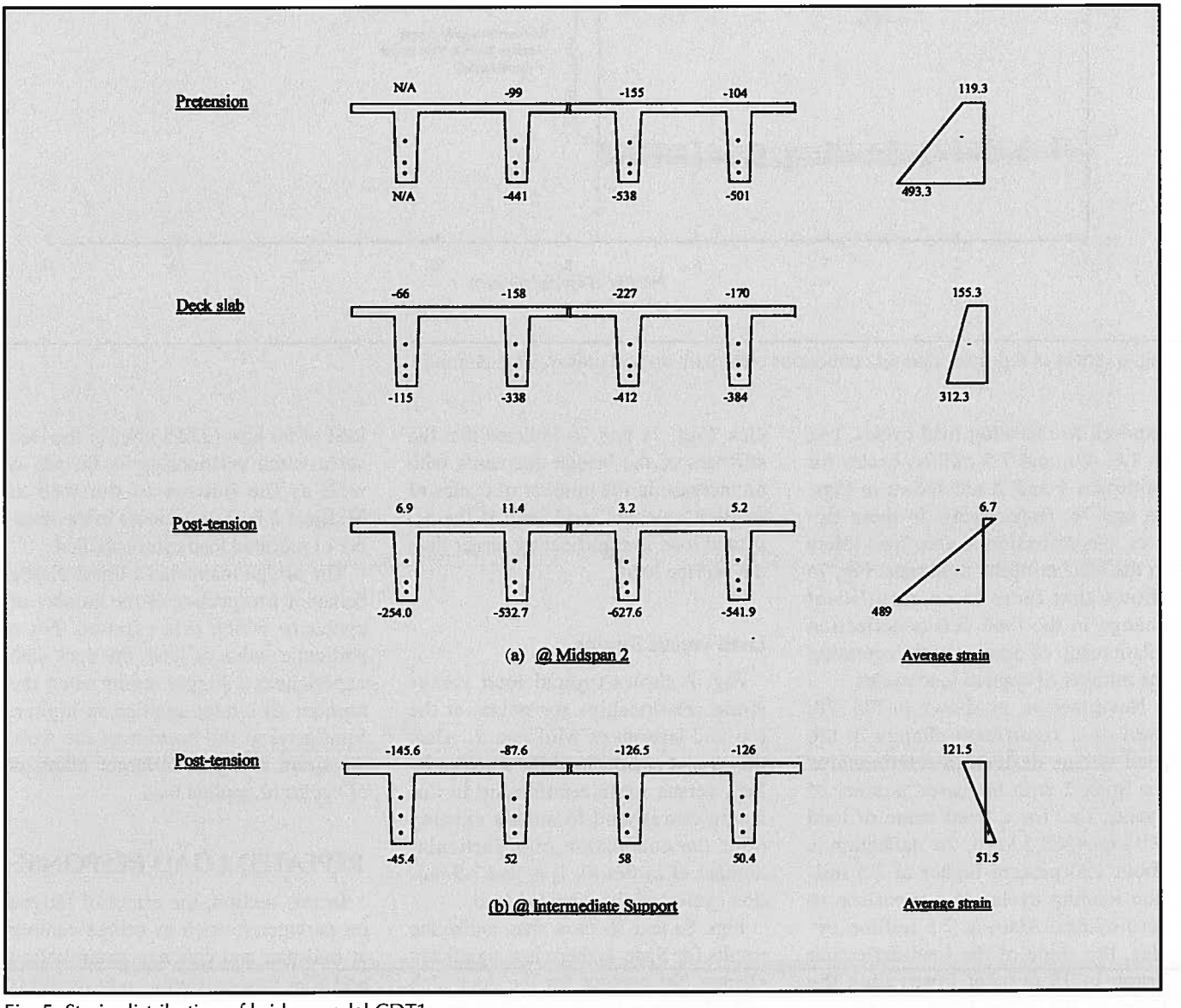

Fig. 5. Strain distribution of bridge model CDT1.

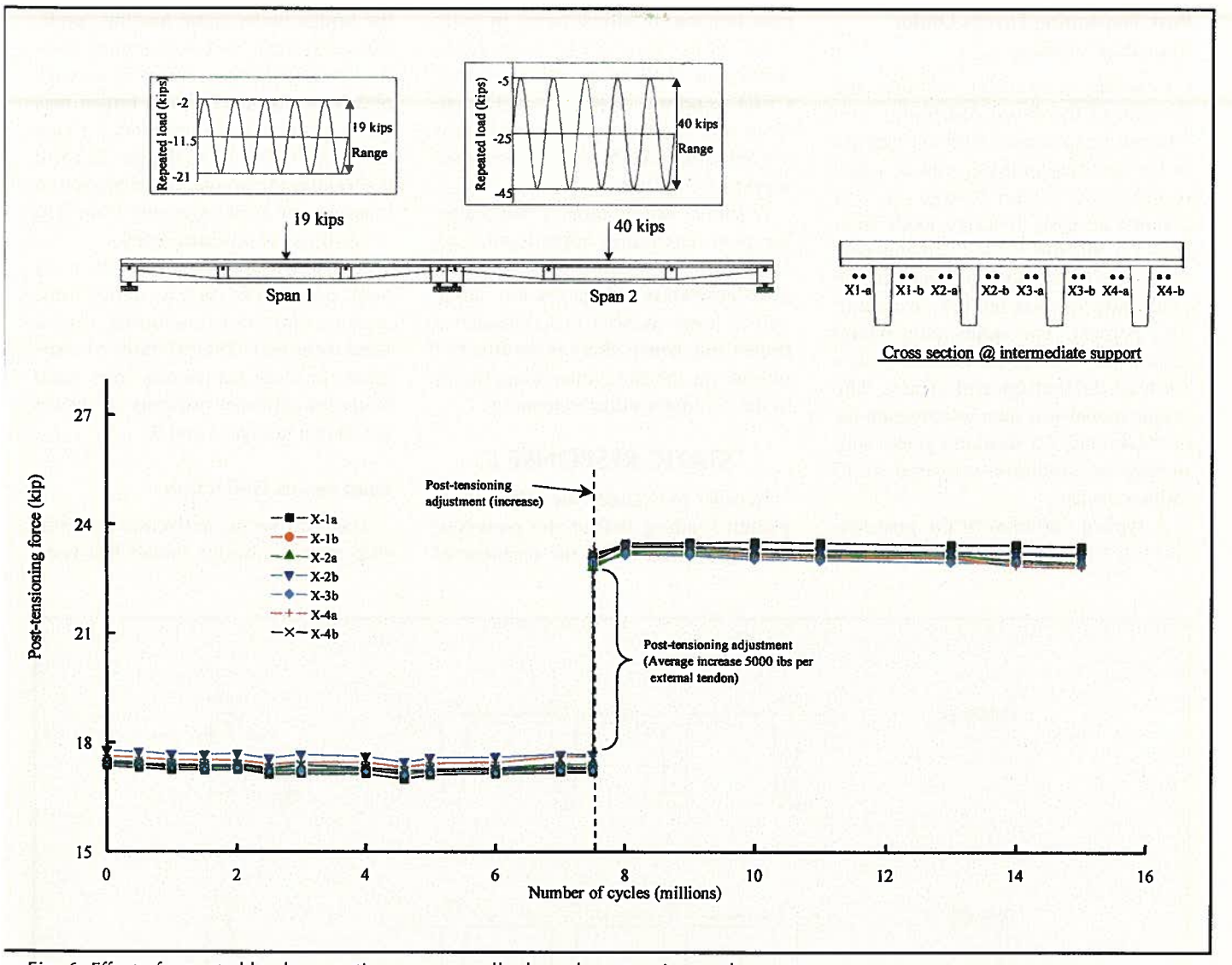

Fig. 6. Effect of repeated load on continuous externally draped prestressing tendons.

exposed to repeating load cycles, i.e., 0, 1.0, 4.0, and 7.5 million cycles for Midspans 1 and 2, are shown in Figs. 7a and 7b, respectively. In these figures, the deflection at zero load refers to the camber of the midspans. Fig. 7a shows that there is no significant change in the load versus deflection relationship of Span 1 with increasing the number of applied load cycles.

Nevertheless, as shown in Fig. 7b, there is a significant change in the load versus deflection relationships for Span 2 with increased number of cycles, i.e., for a fixed value of load [50 kips (222.5 kN)], the deflection is about 150 percent higher at 7.5 million loading cycles in comparison to zero cycles. Also, at 7.5 million cycles, the slope of the load-deflection graph is 33 percent lower than the slope of the same graph at zero cycles. Figs. 7a and 7b indicate that the stiffness of the bridge decreases with an increase in the number of cycles of applied repeated load only if the repeated load is significantly larger than the service load.

Load versus Strains

Fig. 8 shows typical load versus strain relationships for points at the top and bottom of Midspan 2. Also, the strains at zero load for a particular load versus strain relationship in this figure correspond to strains existing after the conclusion of a particular number of cycles (0, 1, 4, and 7.5 million cycles) of the repeated load.

Figs. 8a and 8b show that, unlike the results for Span 1, there is a significant change [90 percent for the deck slab and 67 percent for the web bottom at a load of 50 kips (222.5 kN)] in the load versus strain relationship for the top as well as the bottom of the web at Midspan 2 with an increase in the number of repeated load cycles applied.

The bridge maintains a linear elastic behavior irrespective of the number of cycles to which it is exposed. For a particular value of load, the deck slab experiences a higher strain when the number of cycles applied is higher. Similarly, at the bottom of the web, the strain is higher at larger numbers of cycles of applied load.

REPEATED LOAD RESPONSE

In this section, the effect of fatigue on parameters such as bridge camber at midspan and concrete strain before and after post-tensioning adjustment is discussed.

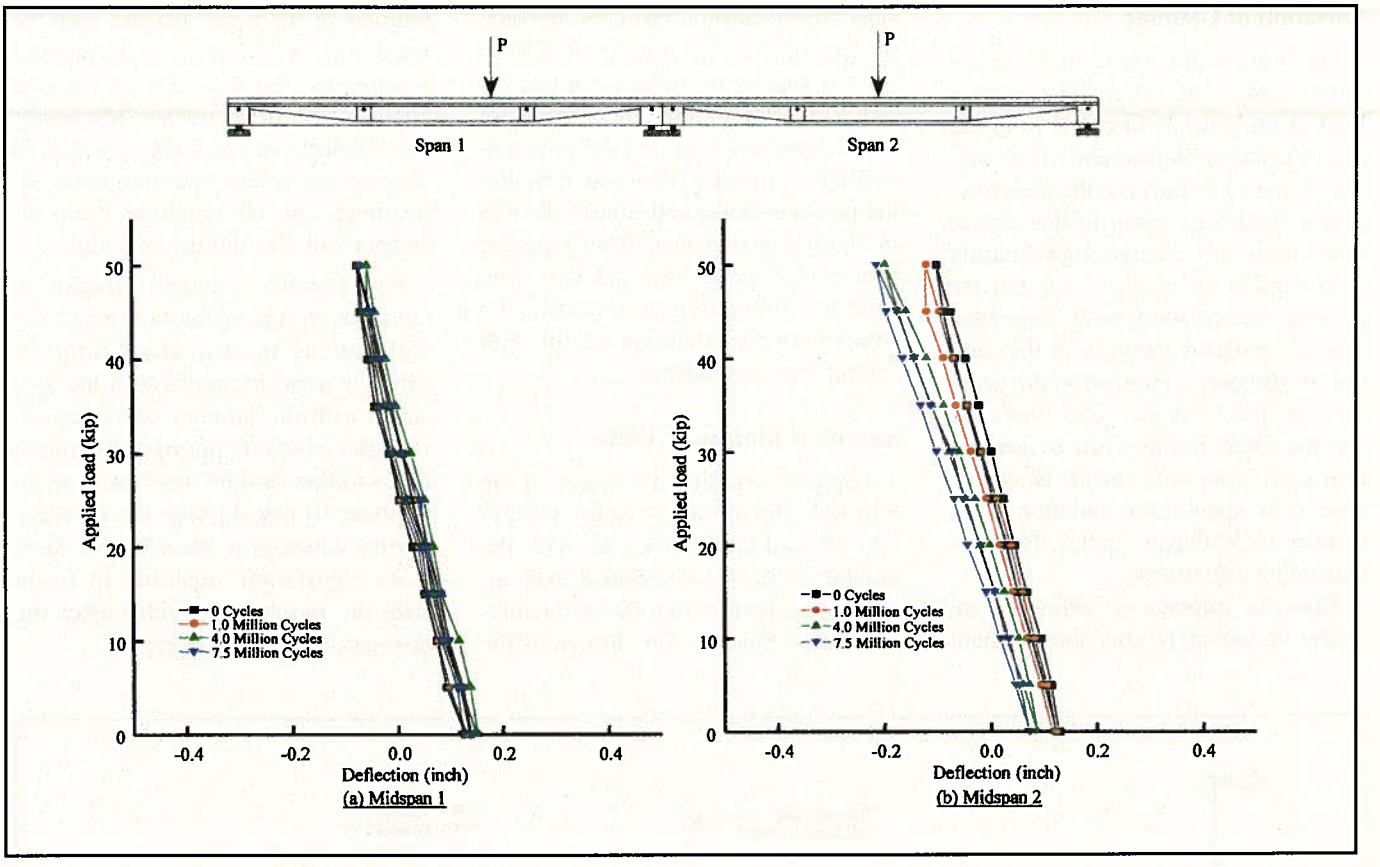

Fig. 7. Deflection at midspans due to static loads.

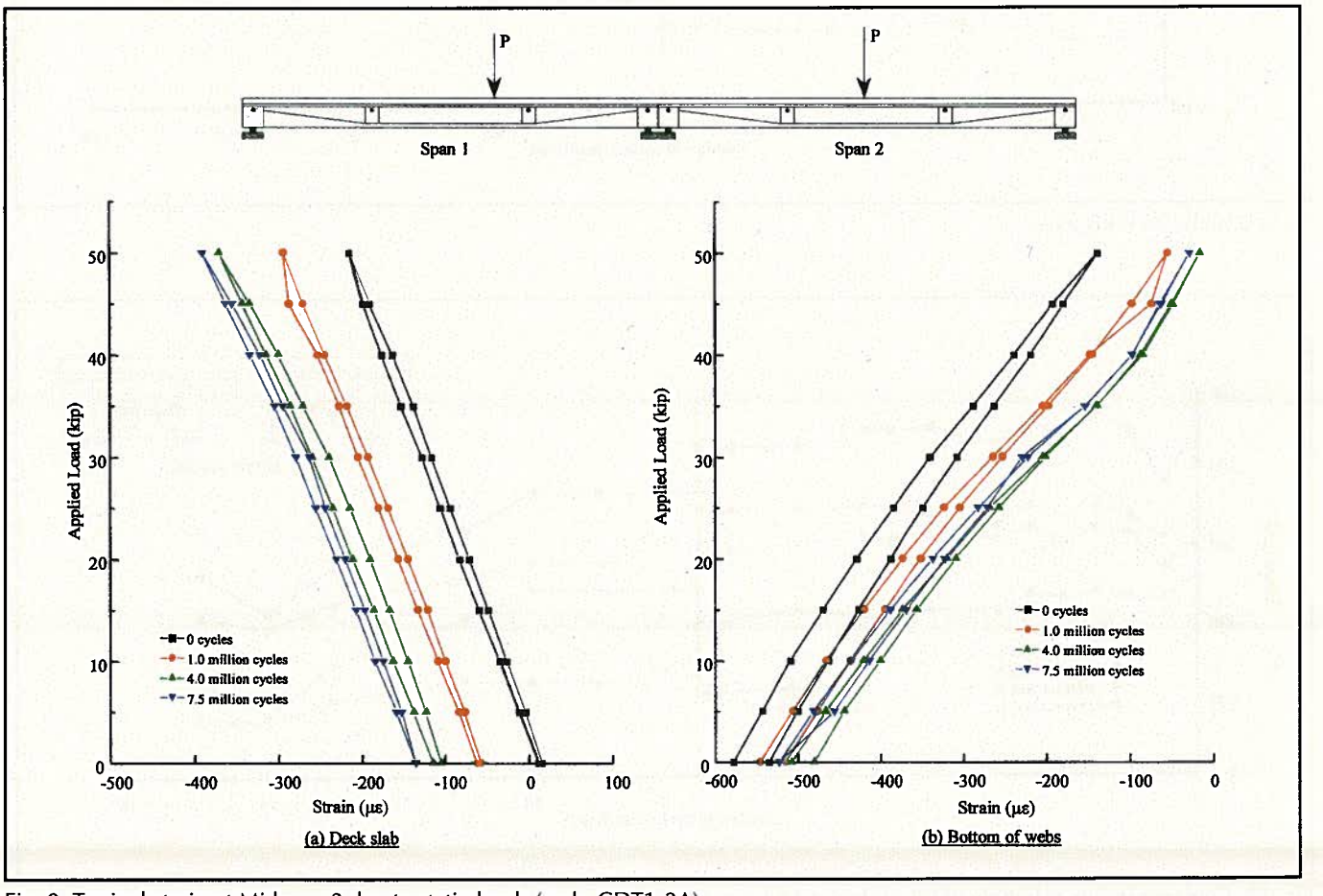

Fig. 8. Typical strain at Midspan 2 due to static loads (web, CDT1-2A).

Variation of Camber

Fig. 9 shows the variation in camber with number of cycles of repeated load at midspan before and after the post-tensioning adjustment. The camber of Span 1 (subject to the lighter repeated load, i.e., equal to the service load) does not change significantly with number of cycles, even after the post-tensioning adjustment. Nevertheless, a significant variation in the camber of Midspan 2 (subject to the heavier repeated load, i.e., two times the service load) is observed before the post-tensioning adjustment. However, there is no appreciable variation in the camber of Midspan 2 after the post-tensioning adjustment.

Thus, the cambers of both spans increase immediately after the post-tensioning adjustment. Obviously, the relationship between the camber at midspan and the number of repeated loading cycles is affected by both the magnitudes of the repeated load and the post-tensioning adjustment. Also, note that after the post-tensioning adjustment, the loss in camber at midspan (from repeated load cycles) is recovered and there is no further appreciable variation in the camber at either midspan section with further repeated loading.

Strains at Bottom of Webs

Typical variations in strains at the bottoms of individual webs (CDT1-3A, 3B and CDT1-4A, 4B) with the number of cycles of repeated load applied are shown in Fig. 10 for the midsection of Span 1. The strains at the bottoms of the webs increase with the number of cycles in the early stage of loading, but reach a constant value at about four million cycles. Moreover, the compressive strain shows a desired increase due to the post-tensioning adjustment, and the concrete strain increases with the number of cycles.

Fig.11 shows a typical variation in concrete strains at the bottom of the webs at the intermediate support. There is a tensile increase in the web strain with the number of cycles before the post-tensioning adjustment and a further desired increase in strain of about 10 percent after the post-tensioning adjustment. Nonetheless, there is no significant variation in strain with the number of cycles after the post-tensioning adjustment.

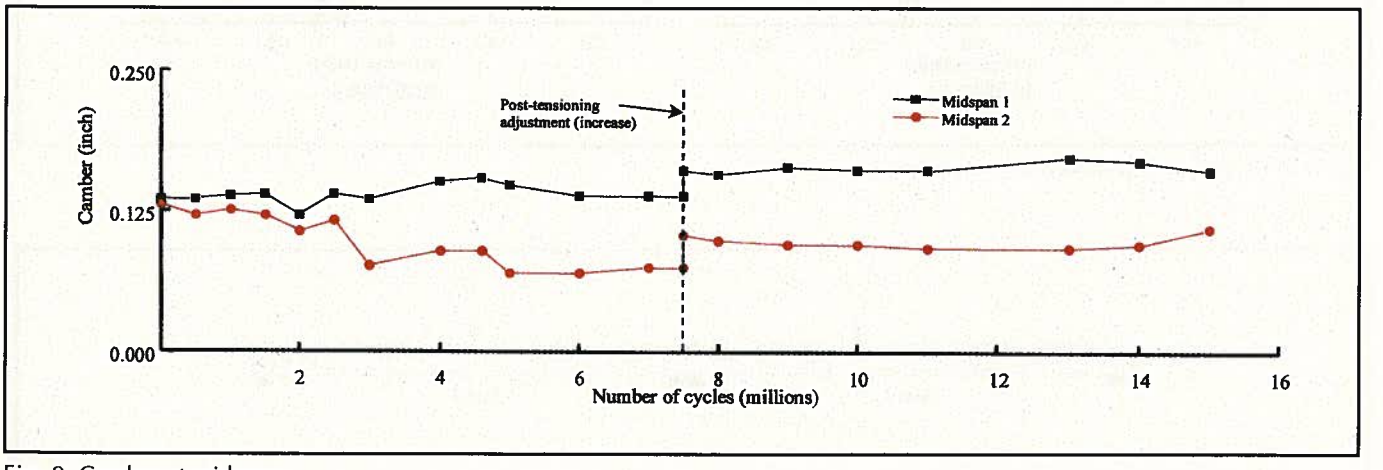

Fig. 9. Camber at midspans.

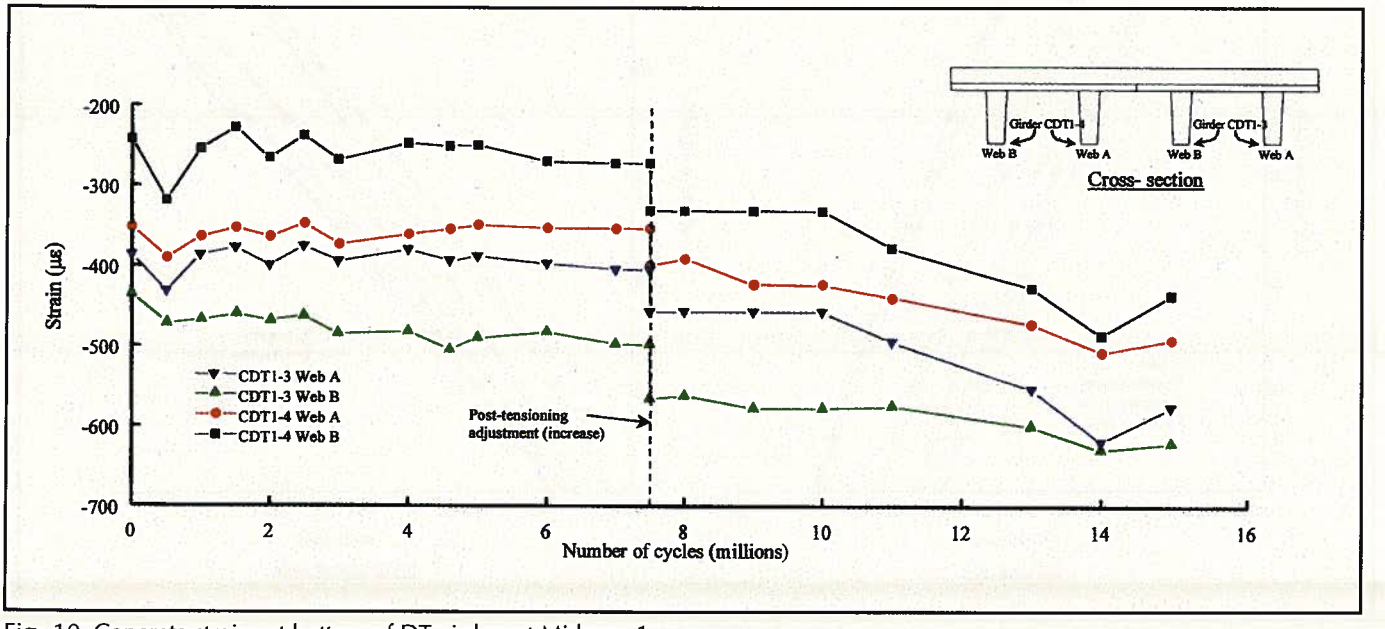

Fig. 10. Concrete strains at bottom of DT girders at Midspan 1.

Strains at Top of Deck Slab

Fig. 12 shows that the variation of strains in the deck slab at the intermediate support is insignificant. However, increasing the post-tensioning forces after 7.5 million cycles resulted in an increase in compressive strains of about 25 percent.

Concrete Strains at Web Bottom

Typical changes in cyclic concrete strains at the bottom of the DT girders at Midspan 2 are shown in Fig. 13. The cyclic compressive strain at the bottom of the DT girder at Midspan 1 is compressive throughout the repeated load cycles, before and after the post-tensioning adjustment. However, the amplitude of the cyclic strain decreases, while the mean value increases after the post-tensioning adjustment.

A similar response is observed for the concrete strain at Midspan 1 (not shown in the figure). The change in the mean value and amplitude of cyclic strain after the post-tensioning adjustment is not as significant as for Span 2. However, the percentage decrease in the amplitude of cyclic compressive strain after the post-tensioning adjustment is the same (i.e., 6 percent) for both midspan sections.

Strain in Deck Slab

Fig. 14 shows typical changes in the cyclic strain in the deck slab model with number of cycles of repeated loads at Midspan 2. This figure suggests that the amplitude of the cyclic strains does not show appreciable variation but that the mean of the cyclic strains is increasing with the number of cycles of applied repeated loads before the post-tensioning adjustment. However, after the post-tensioning adjustment, the mean value of the cyclic strains is reduced drastically.

It is also observed that the amplitude of the cyclic strain has decreased by 12.8 percent with a shift of 144 microstrains in its minimum value. Here, the minimum value of cyclic strain corresponds to the value of cyclic strain at the minimum level of cyclic load.

STATIC RESPONSE II

This section discusses the variation of post-tensioning forces, deflection,

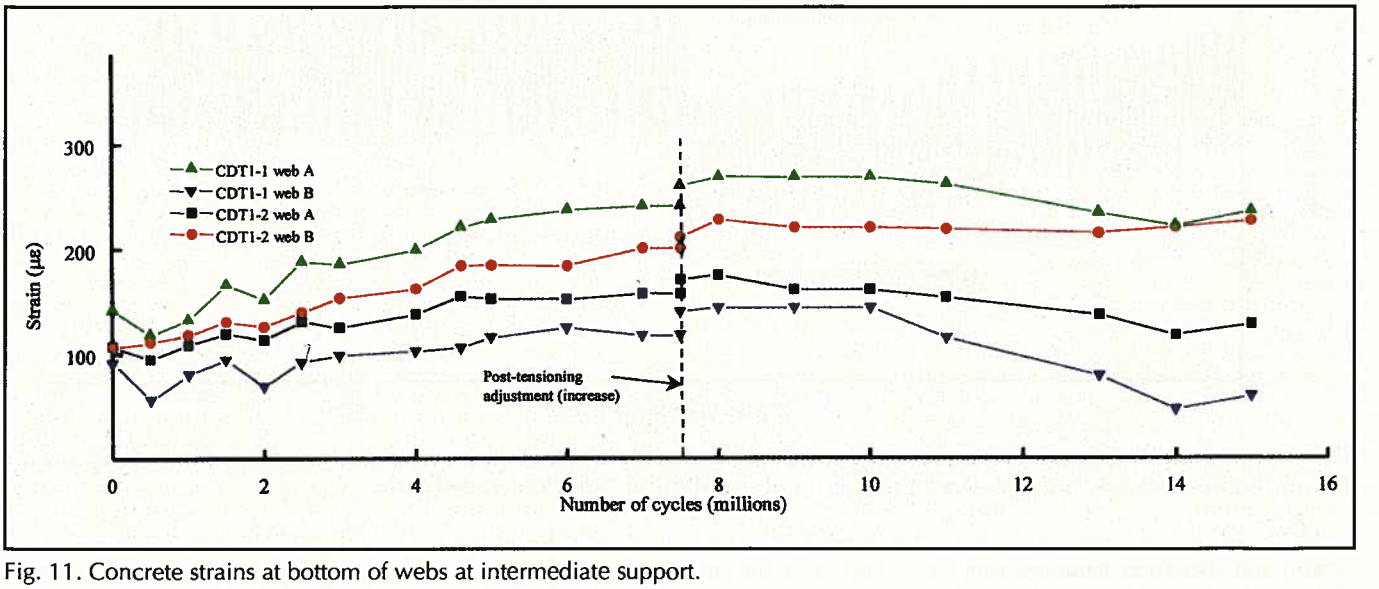

Fig. 11. Concrete strains at bottom of webs at intermediate support.

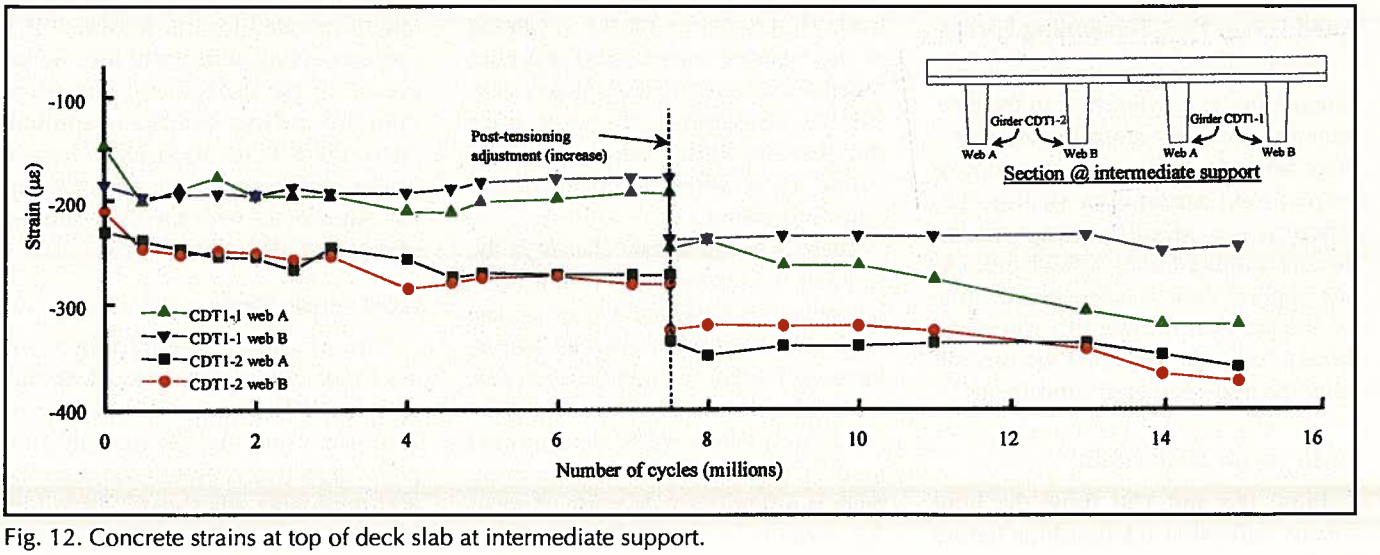

Fig. 12. Concrete strains at top of deck slab at intermediate support.

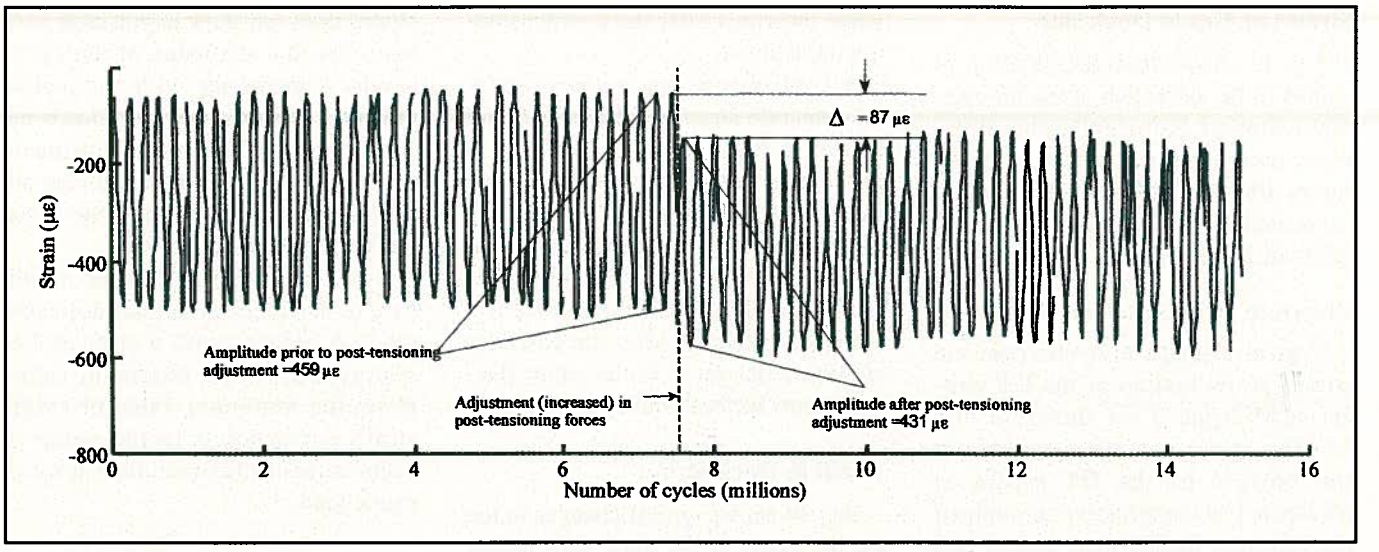

Fig. 13. Typical changes in strain at bottom of DT girder at Midspan 2 due to repeated load.

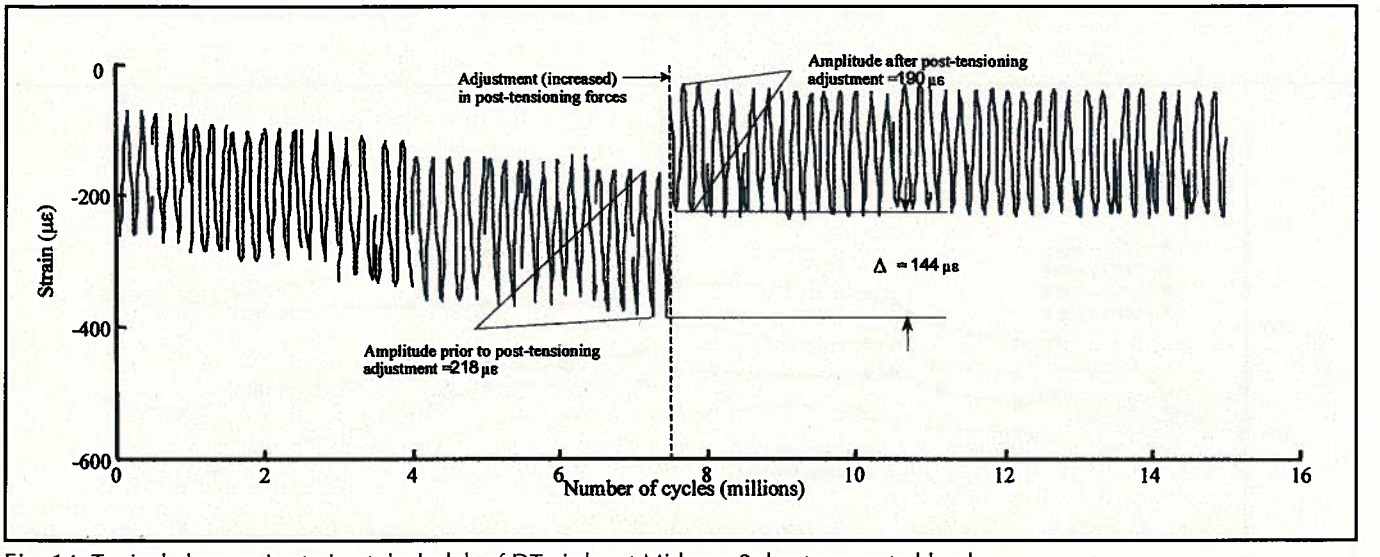

Fig. 14. Typical changes in strain at deck slab of DT girder at Midspan 2 due to repeated load.

strain, and structural behavior due to different loading patterns.

Load versus Post-Tensioning Forces

The load versus average post-tensioning forces relationships in the continuous externally draped tendons before and after the post-tensioning adjustment are shown in Fig. 15. There is a negligible change in the post-tensioning forces with changes in the applied static loading irrespective of the number of cycles to which the bridge has been subjected, before and after the post-tensioning adjustment.

Load versus Deflection

Figs. 16a and 16b show the load versus deflection relationships before and after the post-tensioning adjustment for Midspan 1 and Midspan 2, respectively. The observations were made at zero cycles (at the beginning of the repeated load cycles) and after 7.5 million cycles (before the post-tensioning adjustment). However, after the post-tensioning adjustment, the cyclic loads were continued for another 7.5 million.

There is no significant change in the slope of the load versus deflection relationship with the number of cycles, even after the post-tensioning adjustment, for Span 1 under the service load. However, Fig. 16b shows that for Span 2 subjected to the repeated load of two times the service load, there is a significant decrease of about 33 percent in the stiffness of the bridge at higher numbers of repeated load cycles.

The loss in stiffness of the bridge due to repeated load is recovered if a post-tensioning adjustment (i.e., an increase in the post-tensioning force after 7.5 million cycles) is applied. Also, there is no significant loss in bridge stiffness after the post-tensioning adjustment with the continuation of repeated load cycles.

Load versus Strain

Figs. 17 and 18 show the load versus strain relationships at the deck slab and at the bottoms of the webs for Midspan 1 and the intermediate support, respectively, before and after the post-tensioning adjustment. From Fig. 17a, the compressive strain increases

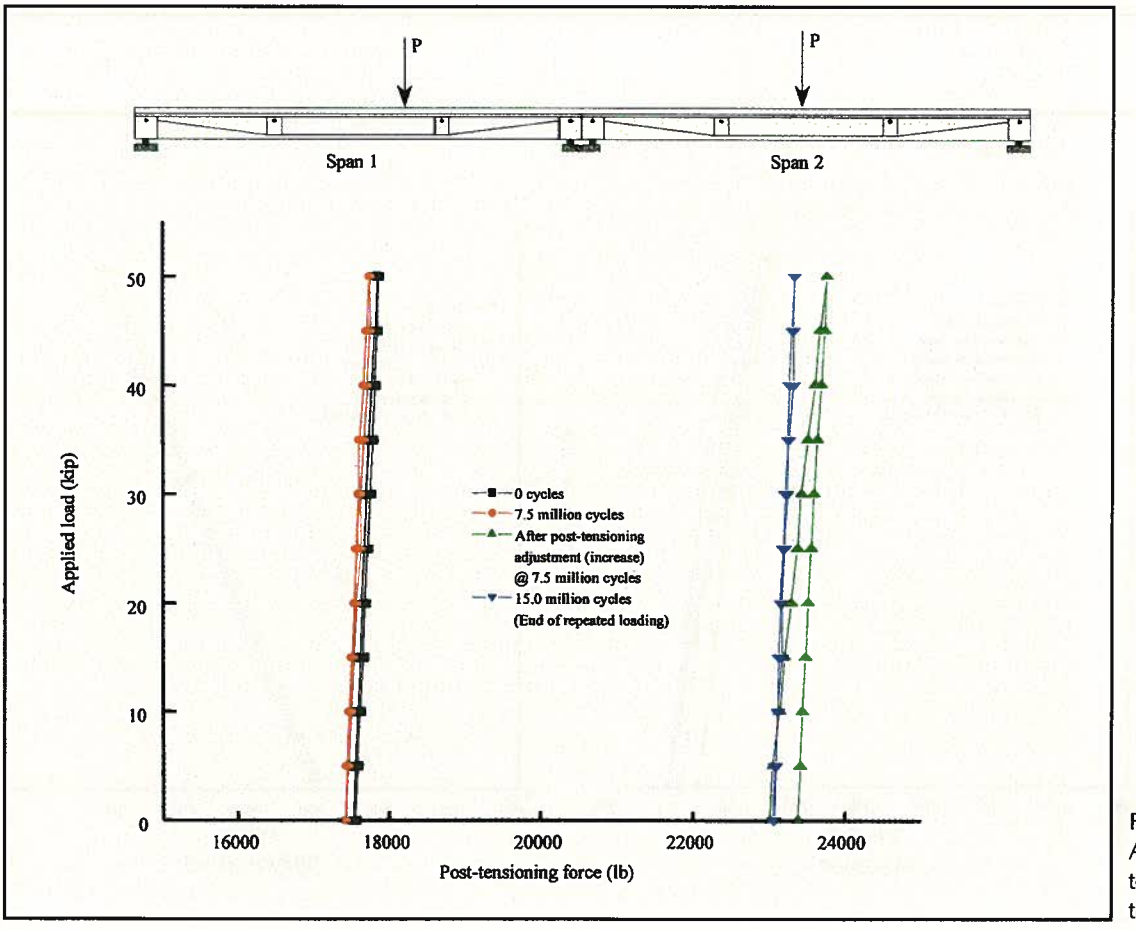

Fig. 15. Average post-tensioning forces due to static load.

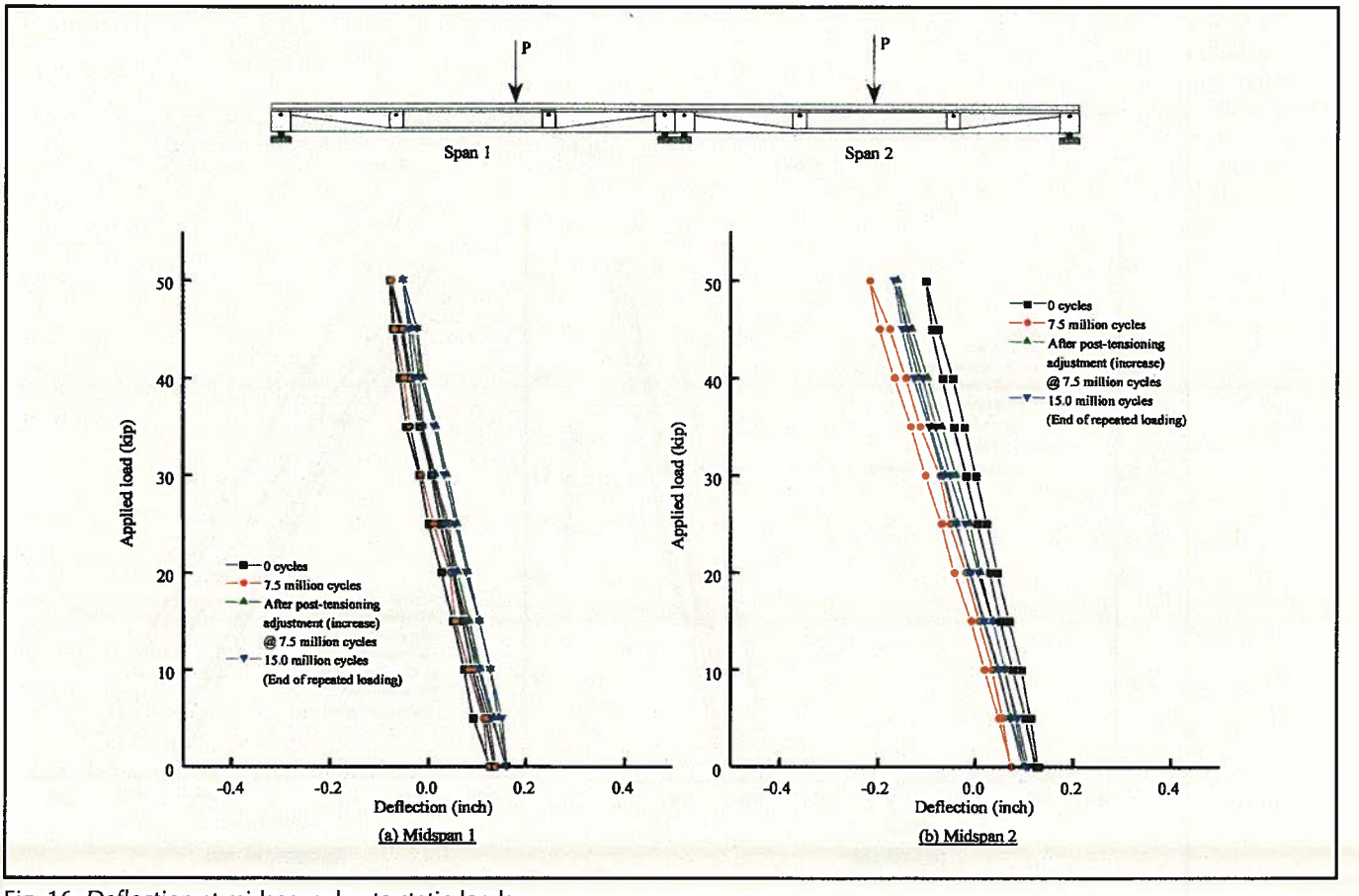

Fig. 16. Deflection at midspans due to static loads.

Fig. 17. Strain variation at Midspan 1 due to static loads.

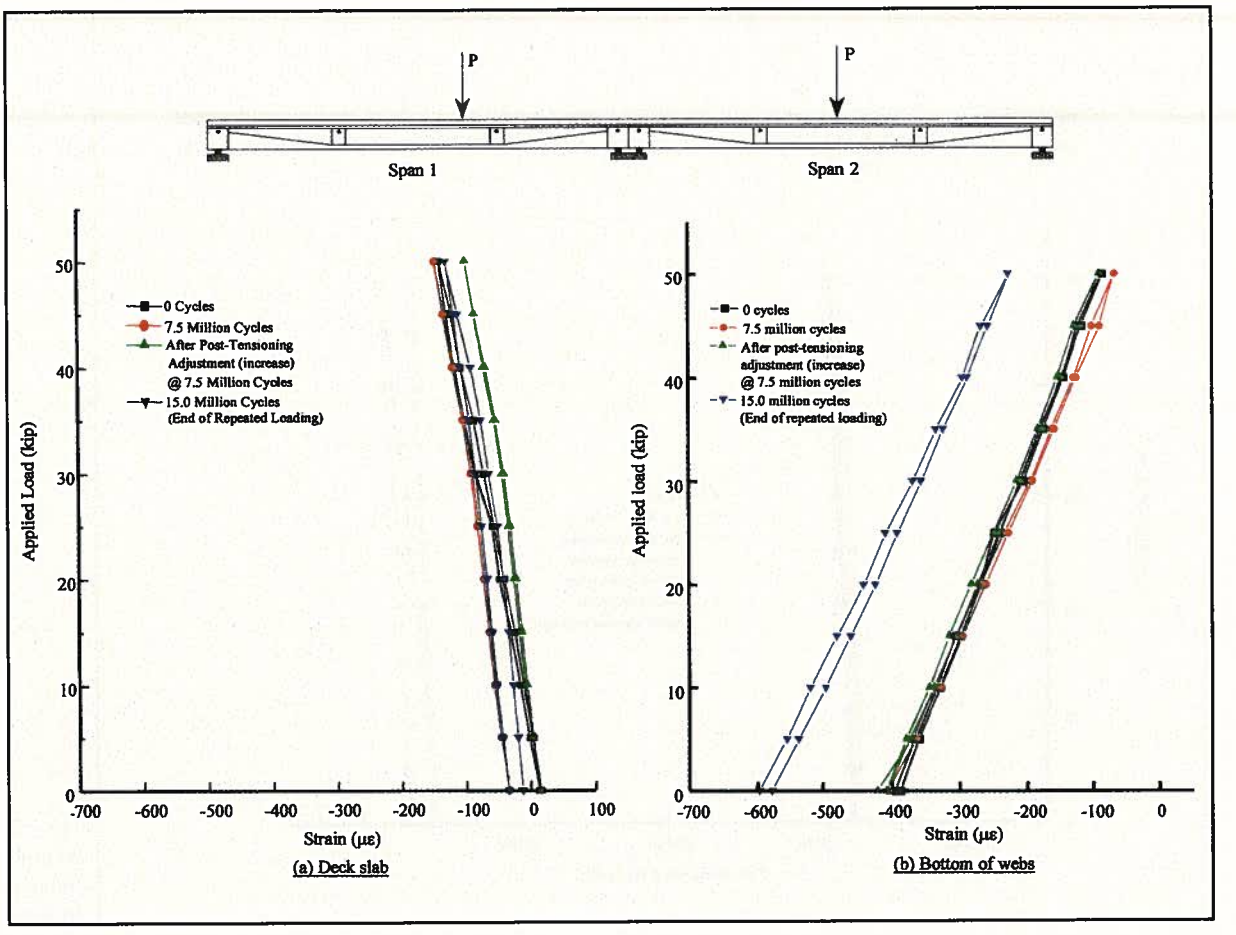

Fig. 18. Strain variation at intermediate support due to static loads.

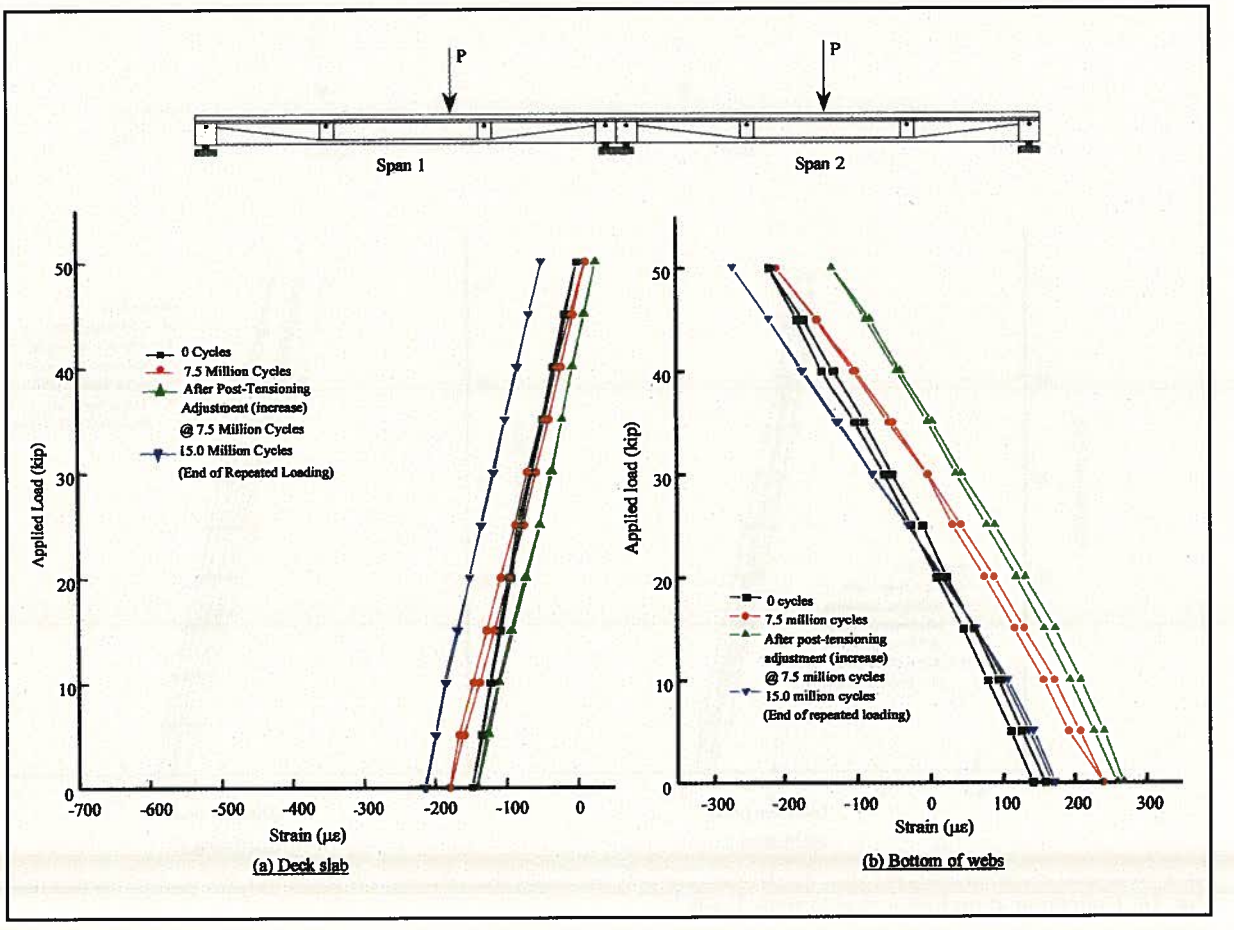

and the tensile strain decreases with increasing load at the deck slab, irrespective of the number of cycles to which the bridge has been subjected. However, the compressive strain at the deck slab (see Fig. 17a) is drastically reduced after the post-tensioning adjustment.

It is shown in Fig. 17b that the load versus strain relationship for the strain at the bottom of the web after the post-tensioning adjustment is almost identical to the relationship before the post-tensioning adjustment. However, a drastic compressive shift in the load versus strain relationship is observed at the end of the repeated loading (i.e., after 15 million cycles). This shift can be attributed to the development of a transverse crack, which formed at a lower number of cycles, across the entire width of the bridge model at the intermediate support. This crack was the result of overloading the bridge model in Span 2 to a load twice its service load for 15 million cycles.

Thus, a very high compressive strain is observed at 15 million cycles compared to the values of strain for other cases of loading cycles for fixed values of load. A significant shift (100 percent) in comparison to other cases of loading cycles in the load versus strain relationship for the deck slab at Midspan 2 (the results are not shown in the figure) is observed for 7.5 million cycles. However, this shift in the load versus strain relationship becomes insignificant after the post-tensioning adjustment has been made.

The post-tensioning adjustment has a long-term effect, which is indicated by the load versus strain relationships after 15 million cycles (see Fig. 17a). The strain at 15 million cycles after the post-tensioning adjustment is close to the strain at zero cycles. Note that the long-term effect, here, refers to the redistribution of the strain with an increase in the number of cycles after the post-tensioning adjustment has been made.

In Fig. 18a, it is shown that in the deck slab at the intermediate support, there is a significant (50 percent) increase in the compressive strain after the post-tensioning adjustment has been made, which continues until the completion of 15 million cycles, irrespective of the magnitude of the static load.

From Fig. 18b, for a fixed value of the load, strains are higher at higher numbers of repeated loading cycles. However, after the post-tensioning adjustment, a redistribution of strain occurs with increasing numbers of repeated loading cycles, and the load versus strain relations at 15 million cycles come closer to those at zero cycles. This redistribution in strains can also be attributed to the wider crack opening at the intermediate support after 15 million cycles of repeated loads.

Response due to Offset Loads

Fig. 19a shows the load distribution before and after the post-tensioning adjustment for various loading cycles of the offset load applied to one web at a time. Fig. 19b shows a similar load distribution when the four-point load is applied at two webs at a time. Here, the load distribution refers to the proportion of the applied load carried by a particular web, expressed as a percentage of the applied load.

The load distribution is determined by expressing the deflection experienced by a particular web as a percent-

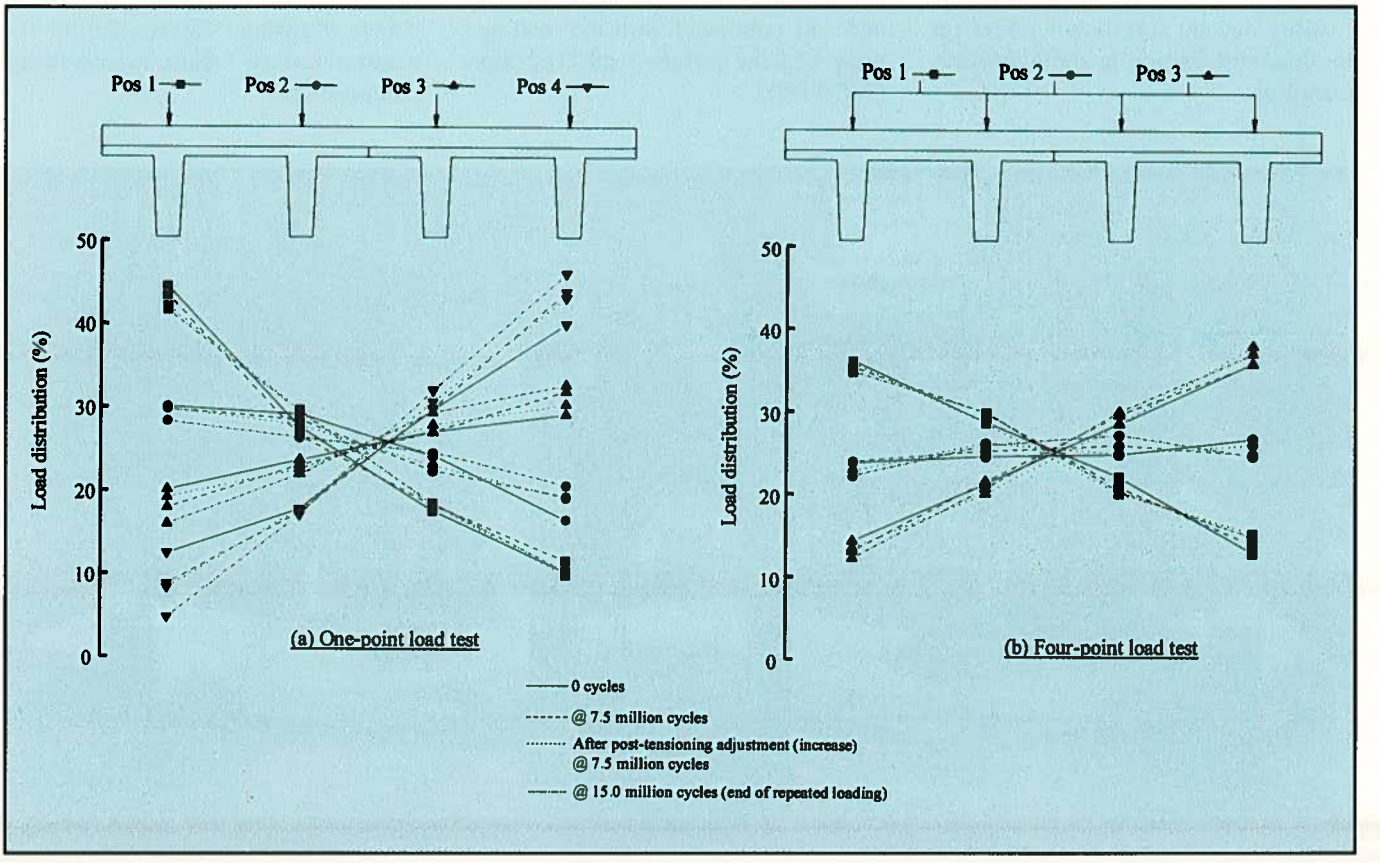

Fig. 19. Load distribution in Span 1.

age of the total deflection of all four webs. From Fig. 19a, the web nearest to the point of load application carries the highest load, i.e., 45 percent of the applied load. The loads carried by the other webs decrease as the distance from the applied load increases.

This response is observed irrespective of the number of repeated load cycles and the post-tensioning adjustment. However, Fig. 19b shows that when the four-point load is applied at Position 1, the load carried by the outer web is higher than the load carried by the inner web even though the point of load application is at the same distance from the two webs. A similar response is shown for Position 3. Note that the slab did not experience any longitudinal cracks at the joint between the two double-tee girders under the eccentric load.

Observations regarding load distribution factors and no longitudinal cracks due to eccentric loading confirm the integrity of the bridge model as a single unit in the transverse direction. Transverse post-tensioning significantly improved the load distribution along the transverse direction by maintaining the continuity of the bridge model. Note that repeated loading had no significant effect on the load distribution in the transverse direction.

ULTIMATE LOAD TEST

To examine the ultimate load carrying capacity, maximum deflections, critical failure sections, modes of failure, variations in post-tensioning forces in the externally draped tendons, and most importantly the ductility of the bridge system, static loads were applied in increments of 5 kips (22.25 kN) at the middle of each span. Deflections along the two spans and along the width at the middle of each span were recorded during the entire test.

To determine the ductility (expressed as the ratio of the total inelastic energy absorbed to the total energy of the system), it was necessary to separate the inelastic energy from the total energy. To evaluate the inelastic energy absorbed in the system, static loading and unloading tests were conducted. In these tests, the load was increased from zero to a maximum value [60, 90, 100, 110, 120, 140, 160 kips (267, 400.5, 445, 489.5, 534, 623, 712 kN), respectively, for the loading/unloading cycles which followed in the sequence] and then unloaded to zero values. Each loading/unloading cycle followed the same procedure and was continued until the load approached the failure load [162 kips (720.9 kN)].

The failure of the bridge system was initiated by crushing of the concrete at the bottom of the webs and significant wide transverse cracks in the deck slab at the junction of Span 2 and the intermediate support. The failure, exactly at the midpoint of the intermediate support, could not occur because of the very high stiffness of the bridge at this section due to the presence of the two cross-beams and the transverse post-tensioned tendons. The failure at the intermediate support was followed by crushing of the concrete in the deck slab at Midspan 2, and then by the rupture of the internal prestressing tendons.

After the failure at Midspan 2, the loading was continued on Midspan 1, which subsequently collapsed at a load of about 165 kips (733 kN). The bridge system after complete failure is shown in Fig. 20. One of the continuous externally draped post-tensioned tendons failed.

Also, wide vertical cracks formed at the hold-down points of the internal tendons. The NEFMAC grids in the webs ruptured at the midspans and intermediate support sections. Plan and elevation views of the failed bridge model are shown in Fig. 21. These diagrams clearly depict the various failure locations and failed components.

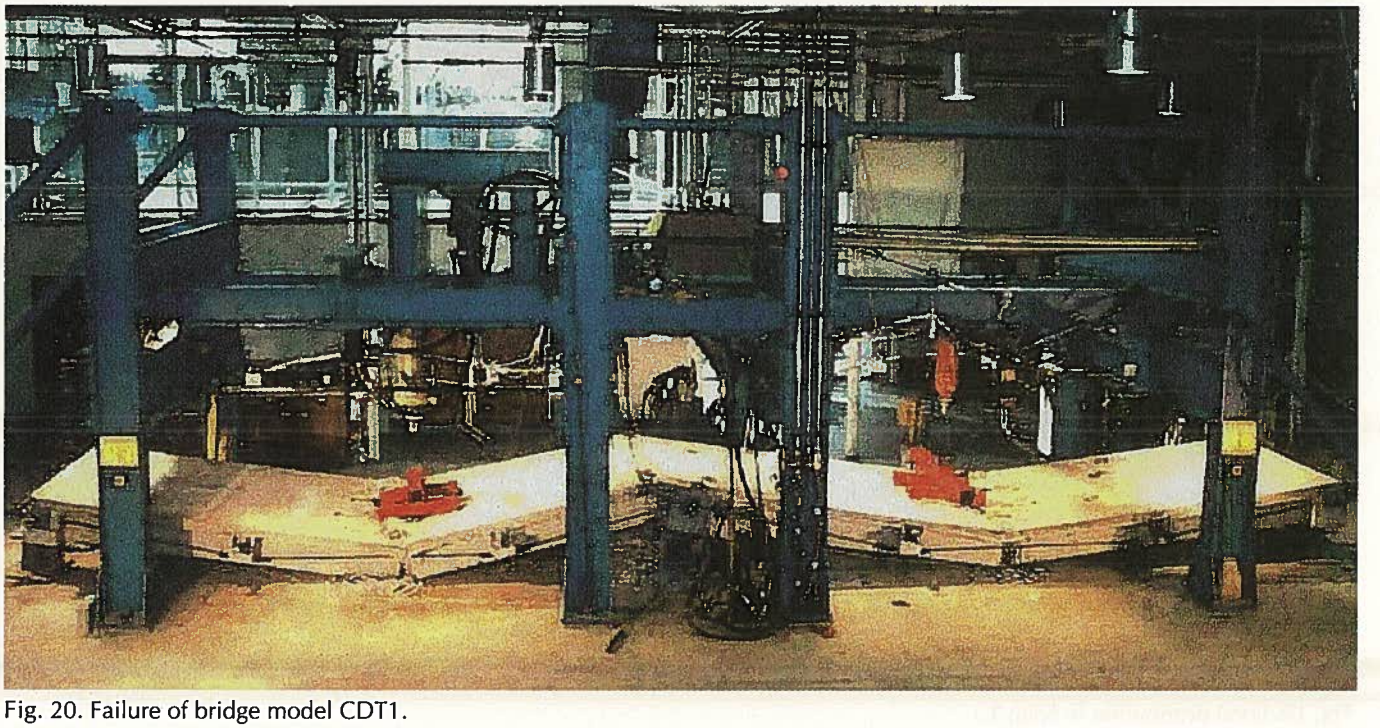

Fig. 20. Failure of bridge model CDT1.

Midspan 2 experienced higher deflections than Midspan 1 at each stage of loading (see Figs. 22 and 23). This difference in responses for the two spans is attributed to the greater repeated load effects on Span 2, which was exposed to a repeated load equal to two times the service load, while Span 1 was subjected to a repeated load equal to the service load.

The first cracks in the bridge appeared in the transverse direction at the intermediate support. These cracks widened as the load was increased. Flexural cracks in the webs occurred in Midspan 2 at a load of 100 kips (445 kN), even though the deflection corresponding to this load was very small, i.e., less than 1.5 in. (38.1 mm) (see Fig. 23).

Measured energy ratios of 80 percent (see Fig. 22) and 86 percent (see Fig. 23) for Midspan 1 and Midspan 2, respectively, indicate that the failure of the bridge was not brittle. These energy ratios are similar to energy ratios that may be experienced by prestressed concrete structures using conventional reinforcements (Grace and Abdel-Sayed[6]). The sequence of rupture of the internal tendons led to a progressive type of failure (see Figs. 22 and 23) after the ultimate load of the bridge was reached.

Prestressing Forces

Fig. 24 shows the applied static load at Midspan 2 versus the prestressing force relationships in the continuous externally draped tendons during the ultimate load test. The post-tensioning forces in the continuous externally draped tendons do not increase significantly during the initial stage of loading. The increase in the post-tensioning forces only becomes significant during the advanced stage of loading, as indicated by the change in the slope of the curves.

This behavior can be attributed to the development of cracks and spalling of the concrete in the bridge. Note that at a load close to the ultimate load of the bridge, there is a further increase in the slope of the curves, except in the case of one tendon for which the reverse trend is observed. This is due to its rupture near the ultimate load of the bridge.

Comparing the responses of this continuous bridge system and a simply supported bridge of the same construction components (Grace and Abdel-Sayed[7]) suggests the following:

- The deflection of the continuous bridge is much smaller, i.e., about 25 percent of that of the simply supported bridge at ultimate load.
- The ductility of the continuous bridge is greater than that of the simply supported bridge, as indicated by a 48 percent (on average) higher value of energy ratio for the continuous bridge.

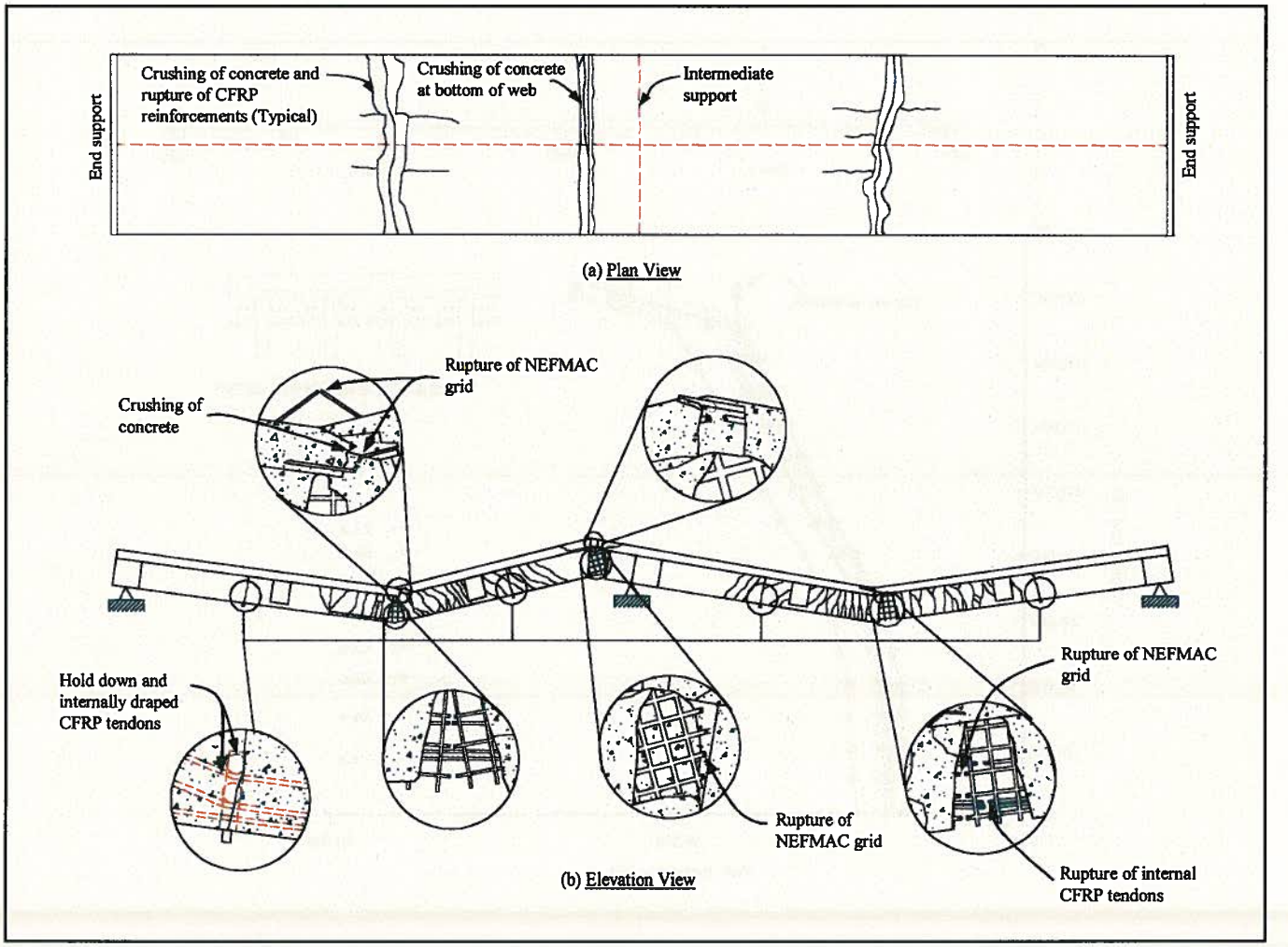

Fig. 21. Failure of bridge model CDT1.

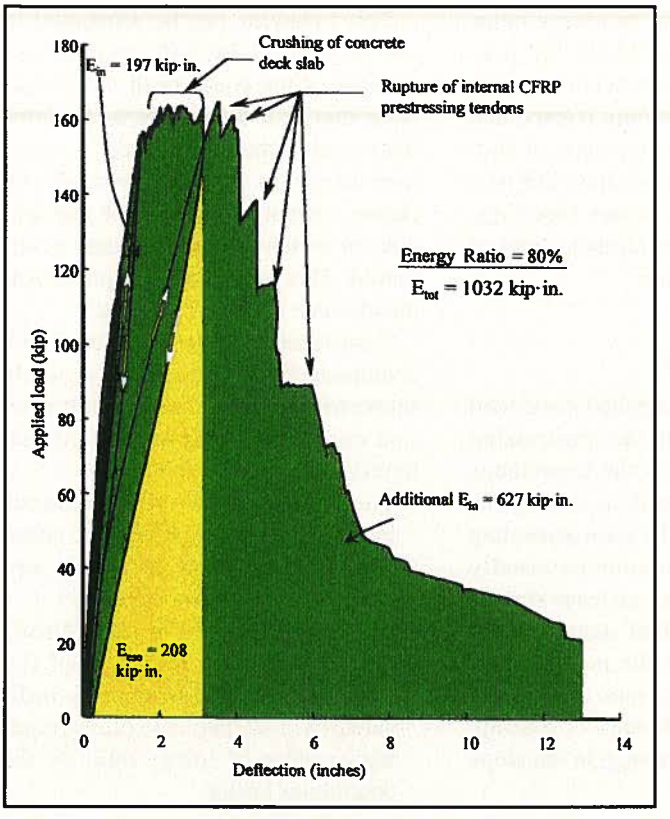

Fig. 22. Energy ratio for Midspan 1.

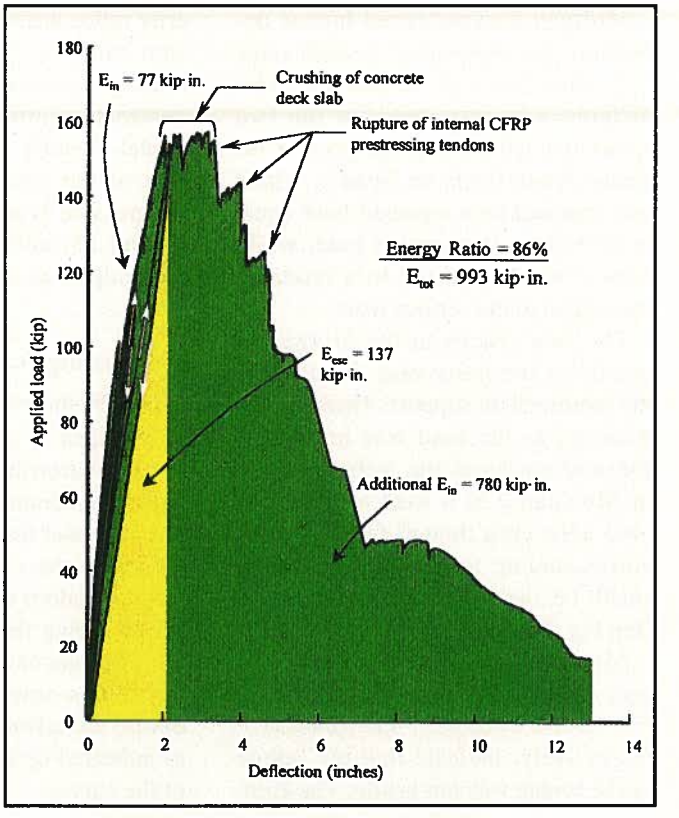

Fig. 23. Energy ratio for Midspan 2.

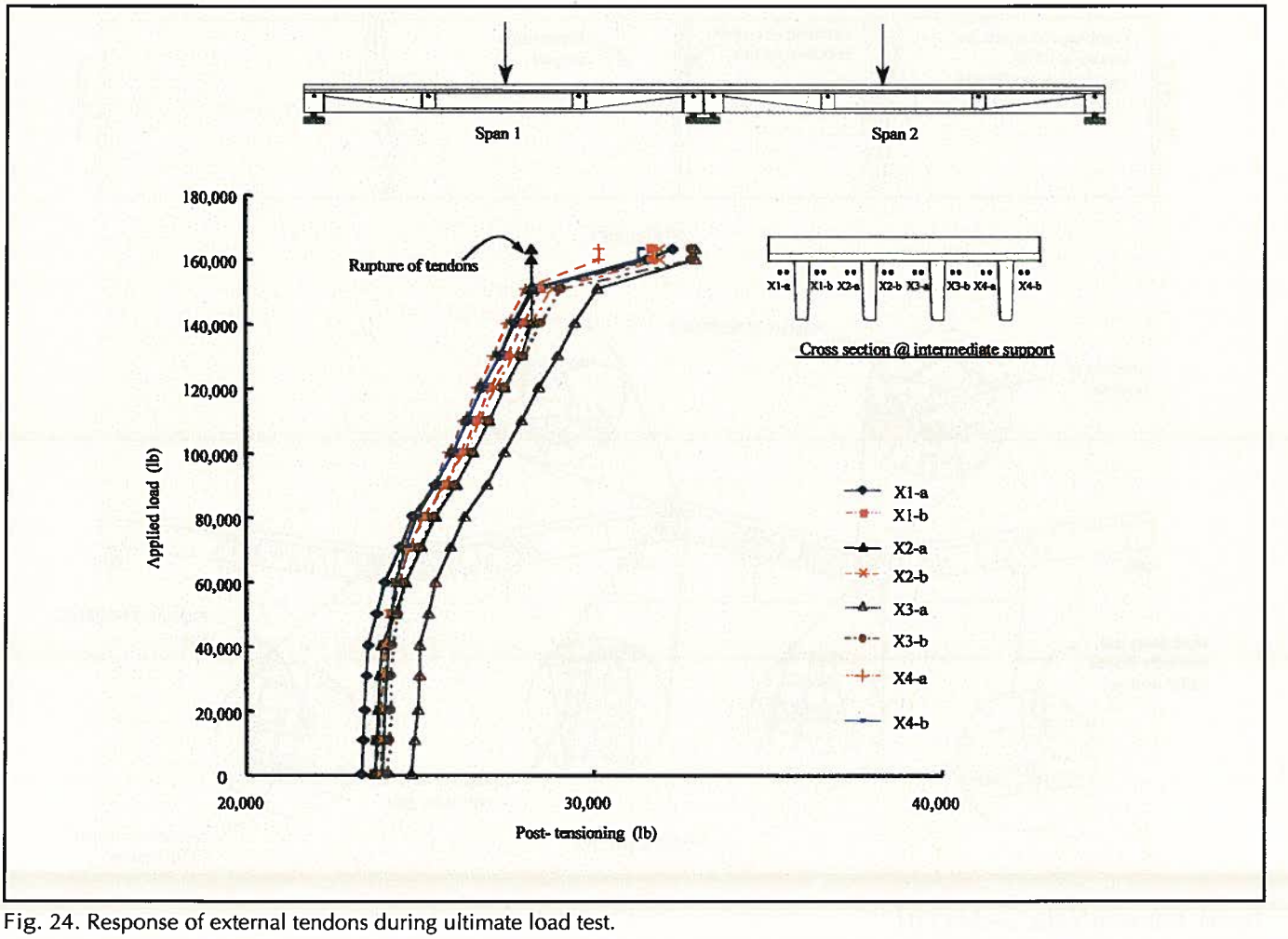

Fig. 24. Response of external tendons during ultimate load test.

- The increase in ductility and the decrease in deflection are attributed to the continuity of the external tendons and the deck slab, as well as the presence of flexural and shear reinforcements in the form of the NEFMAC cage in the webs, deck slab, and flange.
- The increase in post-tensioning forces due to the application of static load to failure in the continuous bridge is not as significant as in the simply supported bridge of the same construction; i.e., there is only an approximate 40 percent increase in post-tensioning forces observed in the continuous bridge, while in the simply supported bridge, post-tensioning forces increased to about twice the initial prestressing value (Grace and Abdel-Sayed[7]).

CONCLUSIONS

Based on the experimental results, the following conclusions can be drawn:

1. There is no significant effect of repeated loading on forces in the post-tensioned externally draped tendons, even with a repeated load of twice the service load. Also, no rupture or even changes in the surface texture of the CFRP tendons at the deviating points in the positive and negative moment regions occurred after 15 million cycles of repeated loads. This provides confidence in the suitability of CFRP tendons for continuous prestressing through the positive and negative moment regions in multispan bridges and their anchor system.

2. The effect of repeated loads on parameters such as deflection and strain depends on the amplitude of the repeated loads and the load history of the bridge. These effects are more significant when the repeated load is significantly greater than the service load.

3. The effect of the post-tensioning adjustment in conjunction with repeated load cycles causes strain reversals (primarily at midspans). The combined effect of these two factors develop beneficial compressive strains throughout the depth of the girders at midspans and compressive (tensile) strains at the top (bottom) of girders at the intermediate support.

4. The overall stiffness of the bridge is reduced with an increase in the number of repeated load cycles at a load of two times the service load before the post-tensioning adjustment. However, this effect is diminished after the post-tensioning adjustment.

5. There is no appreciable variation in the amplitude or the mean of the cyclic concrete strains in the webs with number of cycles of repeated load, both before and after the post-tensioning adjustment. However, the post-tensioning adjustment causes a decrease in the amplitude of approximately 6 percent and an increase (approximately 90 percent) in the mean value of cyclic web strains at midspans. Also, the amplitude of the web strains at the intermediate support is decreased by about 11 percent while the mean value is decreased due to strain reversal (compressive to tensile) at this support.

6. The mean of the cyclic deck slab strains is significantly affected by the number of repeated load cycles before the post-tensioning adjustment, unlike the mean of the web strains. However, after the post-tensioning adjustment, the effect of the repeated load becomes insignificant but the amplitude of cyclic deck slab strain decreases by about 13 percent.

7. There is no appreciable effect of repeated loading on the transverse load distribution factors both before and after the post-tensioning adjustment. The transverse post-tensioning contributed to improve the load distribution factor for the bridge model, making it act as a single structural unit.

8. The presence of continuous externally draped CFRP tendons and CFRP NEFMAC grids, on both sides of the webs and in the continuous deck slab, together with an increase in the level of the external prestressing forces, resulted in a ductile CFRP continuous bridge system.

9. The measured energy ratio for the continuous bridge model was increased by 48 percent, while the maximum midspan deflection at failure was reduced by 75 percent, in comparison to those values of a simply supported bridge using the same construction components.

10. The ultimate load carrying capacity of the two-span continuous bridge is about 1.5 times that of a simply supported bridge using the same construction components. The ultimate load carrying capacity is equal to about eight times the service load.

ACKNOWLEDGMENT

This investigation is supported by a consortium of the National Science Foundation (Grant # CMS-9900809 and 9705235), Wright Patterson Air Force Base, Michigan Department of Transportation (MDOT), the Concrete Research Council of the American Concrete Institute, Holnam, Inc., Mitsubishi Chemical Corporation (MCC), Sumitomo Corporation, Tokyo Ropes Manufacturer, Inc. (TR), and Mitsui Corporation. The support of Dr. VJ. Gopu and Dr. John Scalzi, Program Directors at the National Science Foundation, is greatly appreciated.

This extensive experimental program was made possible by several research associates, graduate and undergraduate students. The tireless and endless work provided by Nate Blackburn is gratefully acknowledged. Technical comments provided by Roger Till (MDOT), Kensuke Yogi (MCC), and Tsuyoshi Enomoto (TR) are appreciated. Finally, the author wants to thank the reviewers of the PCI JOURNAL for their thorough review of the paper and their constructive comments.

REFERENCES

1. ACI Committee 440, "State-of-the-Art Report on Fiber Reinforced Plastic Reinforcement for Concrete Structures," American Concrete Institute, Farmington Hills, MI, 1996, 153 pp.
2. Rizkalla, S. H., "A New Generation of Civil Engineering Structures and Bridges," Proceedings, Third International Symposium on Non-Mettallic (FRP) Reinforcement for Concrete Structures, JCI, V. 1, 1997.
3. Dolan, C. W., "FRP Prestressing in the USA," *Concrete International*, V. 21, No. 10, October 1999, pp. 21-24.
4. Tadros, G., "Provisions for Using FRP in the Canadian Highway Bridge Design," *Concrete International*, V. 22, No. 7, July 2000, pp. 42-47.
5. JCCE, "Recommendations for Design and Construction of Concrete Structures Using Continuous Fiber Reinforcing Materials," Concrete Engineering Series 23, Japan Society of Civil Engineers, Tokyo, Japan, 1997.
6. Grace, N. F., and Abdel-Sayed, G., "Ductility of Prestressed Concrete Bridges Using CFRP Strands," *Concrete International*, V. 20, No. 6, June 1998, pp. 25-30.
7. Grace, N. F., and Abdel-Sayed, G., "Behavior of Externally Draped CFRP Tendons in Prestressed Concrete Bridges," PCI JOURNAL, V. 43, No. 5, September-October 1998, pp. 88-101.
8. Grace, N. F., and Abdel-Sayed, G., "Behavior of Externally/Internally Prestressed Concrete Composite Bridge System," Proceedings of the Third International Symposium on Non-Metallic (FRP) Reinforcement for Concrete Structures (FRPRC), V. 2, Sapporo, Japan, October 1997, pp. 671-678.
9. Grace, N. F., Abdel-Sayed, G., Wabha, J., and Sakla, S., "Mathematical Solution for Carbon Fiber Reinforced Polymer Prestressed Concrete Skew Bridges," *ACI Structural Journal*, V. 96, No. 6, November-December 1999, pp. 981-987.
10. Grace, N. F., and Abdel-Sayed, G., "Double Tee and CFRP/GFRP Bridge System," *Concrete International*, V. 18, No. 2, February 1996, pp. 39-44.
11. Grace, N. F., "Innovative System, Continuous CFRP Prestressed Concrete Bridge," *Concrete International*, V. 21, No. 10, October 1999, pp. 42-47.
12. Mitsubishi Chemical Corporation, "Leadline™ Carbon Fiber Tendons/Bars," *Product Manual*, October 1994.
13. NEFMAC, "Technical Data Collection," Autocon Composites Inc., Canada, pp. 1-10.
14. Grace, N. F., "Transfer Length of CFRP/CFCC Strands for Double-T Girders," PCI JOURNAL, V. 5, No. 5, September-October 2000, pp. 110-126.